Short title: Cytokinin, shoot branching and PIN accumulation

Corresponding author:

Ottoline Leyser

Sainsbury Laboratory Cambridge University

Bateman Street

Cambridge

CB2 1LR

Email: ol235@cam.ac.uk

Cytokinin targets auxin transport to promote shoot branching

Tanya Waldie and Ottoline Leyser

Sainsbury Laboratory Cambridge University

Bateman Street

Cambridge

CB2 1LR

One sentence summary: Cytokinin promotes shoot branching in part by promoting plasma membrane accumulation of PIN3, PIN4 and PIN7 auxin exporters in the shoot.

Author contributions:

T.W. designed, performed and analysed the results of all the experiments, co-conceived the research plans, interpreted the results and wrote the manuscript.

O.L. co-conceived the research plans, interpreted the results and wrote the manuscript.

ORCIDs: T.W. 0000-0001-7760-0950, O.L. 0000-0003-2161-3829

Funding information: This work was funded by the European Research Council (N° 294514 – EnCoDe) and the Gatsby Charitable Foundation (GAT3272C)

Corresponding author email: ol235@cam.ac.uk

ABSTRACT

Cytokinin promotes shoot branching by activating axillary buds, but its mechanism of action in this process is unclear. We have previously shown that a hextuple mutant lacking a clade of type-A Arabidopsis Response Regulators (ARRs) known to act in cytokinin signalling has reduced shoot branching compared to wild type. Since these proteins typically act as negative regulators of cytokinin signalling, this is an unexpected result. To explore this paradox more deeply, we characterised the effects of loss of function of the type-B ARR, ARR1, which positively regulates cytokinin-induced gene expression. The *arr1* mutant has increased branching, consistent with a role antagonistic to the type-A ARRs, but in apparent conflict with the known positive role for cytokinin in bud activation. We show that the *arr* branching phenotypes correlate with increases in stem auxin transport and steady-state levels of the auxin export proteins PIN3 and PIN7 on the plasma membrane of xylem-associated cells in the main stem. Cytokinin treatment results in increased accumulation of PIN3, PIN7 and the closely related PIN4 within several hours, and loss of *PIN3*, *PIN4* and *PIN7* can partially rescue the *arr1* branching phenotype. This suggests there are multiple signalling pathways for cytokinin in bud outgrowth; one of these pathways regulates PIN proteins in shoots, independently of the canonical signalling function of the *ARR* genes tested here. A hypothesis consistent with the *arr* shoot phenotypes is that feedback control of biosynthesis leads to altered cytokinin accumulation, driving cytokinin signalling via this pathway.

INTRODUCTION

Plant developmental plasticity is exemplified by the diversity in shoot forms seen within a species, which are tuned according to environmental conditions. One process underlying this diversity is differential activation of axillary buds throughout the plant's life cycle, which results in diverse shoot branching habits. The hormonal signalling network controlling bud activity involves auxin, strigolactone (SL) and cytokinin (CK), all of which have well-defined physiological roles, although the molecular mechanisms through which they control bud outgrowth are not yet entirely clear (reviewed in Domagalska and Leyser 2011; Teichmann and Muhr 2015). It is well-established that apical dominance, the inhibitory effect imposed by an actively growing shoot apex on axillary buds, is mediated at least in part by the synthesis and movement of auxin from young expanding leaves into the basipetal polar auxin transport stream (PATS) in the main stem (Thimann and Skoog 1933; Ljung *et al.,* 2001). Auxin in the PATS does not enter axillary buds to exert this repression, and thus acts indirectly (Hall and Hillman 1975; Morris 1977; Booker *et al.,* 2003). There is a substantial body of evidence supporting two parallel mechanisms for the indirect action of auxin on axillary bud growth (reviewed in Domagalska and Leyser 2011). One is that auxin in the main stem regulates the synthesis of second messengers that move up into the buds and regulate their activity. The other is that stem auxin influences the establishment of canalised auxin flow out of buds into the PATS. According to this canalisation-based mechanism, auxin movement begins as a weak flux from the bud – an auxin source – into the main stem PATS – an auxin sink. This flux narrows and strengthens due to positive feedback between auxin flux and the auxin transport machinery (Sachs 1981; Prusinkiewicz *et al.,* 2009). This process results in the formation of specialised cell files that conduct auxin from source to

sink, and this is hypothesised to be required for sustained bud activation. The action of SL and CK in bud activation control can be considered in terms of these two models.

In dicots, SL is thought to act via both mechanisms. Auxin up-regulates the transcription of SL biosynthetic genes in the stem and SL can move upward into buds, presumably in the transpiration stream (Foo *et al.,* 2001; Bainbridge *et al.,* 2005; Foo *et al.,* 2005; Johnson *et al.,* 2006; Hayward *et al.,* 2009). There, SL modulates expression of the TEOSINTE BRANCHED1/CYCLOIDEA/PCNA (TCP) family transcription factor *BRANCHED1* (*BRC1*), an inhibitor of shoot branching (Aguilar-Martínez *et al.,* 2007; Poza-Carrion *et al.,* 2007; Braun *et al.,* 2012; Dun *et al.,* 2012). However, high *BRC1* transcript levels are neither necessary nor sufficient for bud inhibition and mutant buds lacking *BRC1* can be inhibited by SL (Seale *et al.,* 2017). Furthermore, SL addition can promote branching in an auxin transport compromised genetic background, demonstrating that this simple second messenger mechanism cannot be the only mode of action for SL (Shinohara *et al.,* 2013). Consistent with this idea, SL triggers rapid removal of the auxin export protein, PIN1, from the plasma membrane (Crawford *et al.,* 2010; Shinohara *et al.,* 2013; Bennett *et al.,* 2016). This effect is sensitive to inhibitors of clathrin-mediated endocytosis, but not to the translation inhibitor cycloheximide, suggesting a non-transcriptional mode of action of SL on PIN1 endocytosis. In the context of an auxin transport canalisation-based model for bud activation, PIN1 removal can account for the inhibitory effect of SL on shoot branching since it is predicted to make canalisation more difficult to achieve by dampening the feedback between auxin flux and auxin transporter accumulation. Furthermore, when auxin transport is compromised and

auxin fluxes are systemically low, the effect of SL on PIN1 endocytosis is predicted to promote branching, as observed (Shinohara *et al.,* 2013).

Half a century before the discovery of SL, one of the earliest described roles for CK in plant development was in bud activation (Wickson and Thimann 1958). In Arabidopsis (*Arabidopsis thaliana*), basally applied CK can overcome the inhibitory effects of apical auxin on bud activity (Chatfield *et al.,* 2000). Furthermore, *isopentenyl transferase* (*ipt*) *3,5,7* mutants impaired in CK biosynthesis have reduced CK levels and form fewer branches than wild-type plants (Miyawaki *et al.,* 2006; Müller *et al.,* 2015). As for SL, there is good evidence that CK can act as a second messenger for stem auxin. Removal of the shoot apex correlates with increased stem CK levels, and addition of auxin reduces them (Bangerth 1994; Tanaka *et al.,* 2006). In Arabidopsis, CK is perceived at the endoplasmic reticulum by the HISTIDINE KINASE (AHK) receptor kinase family, which initiate a phosphorelay cascade that targets the large, multi-member family of RESPONSE REGULATORs (ARRs) in the nucleus via HISTIDINE PHOSPHOTRANSFER (AHP) proteins (for review see Schaller *et al.,* 2015). The ARRs possess an N-terminal phosphoreceiver domain and comprise two sub-classes based on the presence (in type-Bs) or absence (in type-As) of a DNA-binding domain. Type-B ARRs directly regulate transcription and function as positive regulators of CK signalling, whereas type-A ARRs typically function as negative regulators. It has therefore been widely assumed that CK activates buds by regulating the transcription of relevant genes in the bud, such as *BRC1*. There is good evidence to support this model since in both pea (*Pisum sativum*) and Arabidopsis, *BRC1* expression is down-regulated by CK (Braun *et al.,* 2012; Dun *et al.,* 2012; Seale *et al.,* 2017). However, CK can promote

bud activation in pea *brc1* mutants, demonstrating that CK has *BRC1*-independent effects on the regulation of bud outgrowth (Braun *et al.,* 2012). Furthermore, the Arabidopsis hextuple type-A *arr3,4,5,6,7,15* mutant exhibits reduced bud activation, a phenotype opposite to that predicted, based on the established roles of type-A ARR proteins as negative regulators of transcriptional CK signalling (To *et al.,* 2004a; Müller *et al.,* 2015).

To explore this paradoxical result further, we describe here the analysis of the type-B *ARR* mutant, *arr1*. ARR1 binds to the promoters of CK up-regulated genes, including those induced during CK-triggered bud activation. We therefore hypothesised the *arr1* mutant should show reduced and CK-resistant shoot branching. However, our results demonstrate *arr1* has increased and CK-responsive shoot branching, suggesting an alternative mechanism for CK-mediated shoot branching control. We provide evidence that the mechanism involves CK-mediated accumulation of the PIN3, PIN4 and PIN7 auxin transporters.

RESULTS

Type-A and type-B *arr* mutations confer opposite shoot branching and auxin transport phenotypes

Previously, we found that the hextuple type-A *arr3,4,5,6,7,15* mutant has reduced shoot branching relative to wild type (Müller *et al.,* 2015). Since type-B *ARR* family members are known to act antagonistically to type-A *ARRs* in other CK responses, we investigated shoot branching in the *arr1* loss-of-function mutant. *ARR1* was selected because a group of CK-up-regulated genes in buds possess an *ARR1* response element in their promoters (Müller *et al.,* 2015). In accordance with action antagonistic to type-A *ARR*s, the type-B *arr1* single mutant has increased branching compared to wild-type controls, forming a mean of 6.8 rosette branches compared to 5.5 in wild type when decapitated (Fig. 1A; $p < 0.001$), and a mean of 6.8 branches compared to 5.7 in wild type when intact (Fig. 1B-E; $p < 0.001$).

Buds on isolated nodal stem segments from *arr3,4,5,6,7,15* plants treated with apical auxin were previously shown to be resistant to the effects of basal CK and slightly resistant to basal SL (Müller *et al.,* 2015). The same isolated nodal assay system was used to assess bud hormone responses in *arr1* (Chatfield et al., 2000; Crawford et al., 2010). Briefly, small nodal stem segments, each bearing an inactive cauline bud, were excised from bolting inflorescences. The apical end of the stem was embedded in an agar block supplemented with synthetic auxin (1-napthalene acetic acid; NAA) or a control solution. The basal end of the stem was embedded in an agar block supplemented with CK (6-benzylaminopurine; BA), SL (*rac*-GR24) or a control solution (hereafter referred to as apical NAA, basal BA and basal GR24

treatments). The kinetics of outgrowth in mock-treated *arr1* buds was similar to wild type (Fig. 2A & B). For both genotypes, apical NAA delayed bud activation by approximately three days. The response of *arr1* to BA was also similar to wild type, where basal BA alone had little effect compared to mock treatment, but basal BA could overcome the inhibitory effect of apical NAA and activate buds. As previously reported, basal GR24 prolonged the inhibitory effect of apical NAA in wild type, but *arr1* buds were resistant to basal GR24 under these conditions (Fig. 2C & D). To assess whether this altered GR24 response extended beyond isolated nodes, whole plants were grown under axenic conditions on ATS media supplemented with GR24, as per Crawford *et al*. (2010). Branching in wild-type plants was significantly inhibited by 1 µM GR24, whereas 5 µM was required for significant branch inhibition in *arr1* plants (Fig. S1).

The altered GR24 responses of *arr1* single and *arr3,4,5,6,7,15* hextuple mutants raise the possibility that *arr* mutations may affect auxin transport processes in the shoot. We therefore compared bulk auxin transport in wild type, type-A and type-B *arr* mutant stem segments, as previously described (Bennett *et al.,* 2016). Compared to wild type, *arr1* transported 40% more auxin ($p < 0.01$) and *arr3,4,5,6,7,15* transported 23% less ($p < 0.01$) over the 6-hour assay period (Fig. 3A). To determine whether this effect was associated with CK signalling, we also assessed the *ipt3* CK biosynthesis mutant, which we have previously shown to have a reduced shoot branching phenotype (Müller *et al.,* 2015). Similar to *arr3,4,5,6,7,15*, the *ipt3* mutant also exhibited reduced auxin transport (Fig. S2). Thus, the degree of shoot branching positively correlates with bulk auxin transport in the stems of these mutant genotypes.

To test this correlation further, we assessed the shoot branching response of *arr1* and *arr3,4,5,6,7,15* plants to the auxin transport inhibitor 1-naphthylphthalamic acid (NPA). Plants were grown under axenic conditions on ATS media supplemented with NPA, as per Bennett *et al*. (2006). Significant reductions in branching were observed in *arr1* plants treated with 0.1 µM NPA ($p < 0.05$) and 1.0 µM NPA ($p < 0.001$) (Fig. 3B), consistent with a causative link between auxin transport defects and shoot branching in the *arr1* mutant, similar to the results obtained for SL deficient mutants (Bennett *et al.,* 2006). In contrast, treatment with 0.1 µM NPA significantly increased branching in *arr3,4,5,6,7,15* ($p < 0.01$) (Fig. 3C). This is consistent with the well-established promotive effect of very low auxin transport on branching (Ruegger *et al.,* 1997; Geldner *et al.,* 2003). Taken together, the results suggest mutations in type-A and type-B *ARR* family members perturb auxin transport in the shoot, and this contributes to their effects on shoot branching.

CK signalling targets PIN proteins in the stem

Several PIN proteins contribute to stem auxin transport in Arabidopsis. PIN1 is an important component of the classical PATS and is expressed in a highly polar manner in xylem parenchyma and cambium cells in the stem vasculature. PIN3, PIN4 and PIN7 contribute to PATS and to a less-polar route, termed Connective Auxin Transport (CAT), which connects surrounding tissues and organs, including axillary buds, to the PATS (Bennett *et al.,* 2016). To determine whether *arr* mutant shoots have alterations in PIN accumulation we analysed the steady-state transcript levels of *PIN1*, *PIN3*, *PIN4* and *PIN7* in *arr1* and *arr3,4,5,6,7,15*. *PIN* transcript levels were analysed in upper inflorescence internodes of wild-type, *arr1* and

arr3,4,5,6,7,15 plants using RT-qPCR (Fig. S3). Apart from a 5-fold increase in *PIN7* transcripts in *arr3,4,5,6,7,15* compared to wild type ($p < 0.01$), no significant changes were observed, suggesting the *arr* mutant auxin transport phenotypes do not correlate with alterations in *PIN* transcript abundance in inflorescence stems.

In the absence of correlative changes in *PIN* transcription, we assessed PIN protein localisation and abundance using established PIN-GFP reporter lines crossed into the type-A and B *arr* mutant backgrounds. PIN-GFP accumulation patterns were analysed in longitudinal or transverse sections of basal inflorescence internodes (the inflorescence internode located directly above the rosette and farthest from the shoot apex) and imaged using confocal microscopy. In *arr3,4,5,6,7,15* mutants, the amount of PIN1-GFP on the basal plasma membrane (the rootward-facing membrane farthest from the shoot apex) of xylem parenchyma cells was unchanged compared to wild type (Fig. 4A-C). In contrast, the amount of PIN3-GFP on the basal plasma membrane of xylem parenchyma cells was reduced by approximately 25% in *arr3,4,5,6,7,15* compared to wild type ($p < 0.001$) (Fig. 4D-F). As PIN7-GFP typically shows a broad, cross-stem pattern of accumulation in young wild-type internodes, and PIN7-GFP was not detectable on the basal plasma membrane of xylem parenchyma cells in *arr3,4,5,6,7,15*, the PIN7-GFP signal was quantified within vascular bundles in inflorescence stem transverse sections (Fig. 4G-I). Like PIN3-GFP, PIN7-GFP was also significantly decreased in *arr3,4,5,6,7,15* compared to wild-type ($p < 0.001$). Analysis of the *ipt3* CK synthesis mutant revealed similar patterns of PIN1-GFP and PIN7-GFP accumulation as the *arr3,4,5,6,7,15* mutant, with wild-type levels of PIN1-GFP present on the basal plasma membrane of xylem

parenchyma cells and decreased levels of PIN7-GFP within vascular bundles ($p < 0.001$) (Fig. S4).

Wild-type levels of basal plasma membrane-localised PIN1-GFP were also observed in the *arr1* mutant (Fig. 5A-C). However, in contrast to *arr3,4,5,6,7,15*, PIN3-GFP was increased approximately 20% in *arr1* inflorescence stems compared to wild type ($p < 0.05$) (Fig. 5D-F). In transverse sections of young basal *arr1* inflorescence internodes (8-10 cm high), PIN7-GFP was restricted to the outer xylem parenchyma and cambium of vascular bundles, whereas wild-type plants exhibited a brighter and broader accumulation pattern that decreased at later stages, as previously reported (Bennett *et al.,* 2016) (Fig. S5). In contrast, the accumulation of PIN7-GFP associated with vascular bundles appeared to be slightly higher in *arr1* than wild type at later stages of inflorescence development (18-20 cm and 28-30 cm high) (Fig. S5C-F). In accordance with this observation, the amount of PIN7-GFP present on the basal plasma membranes of xylem parenchyma cells in longitudinal sections of inflorescence stems was increased approximately 25% ($p < 0.01$) in *arr1* compared to wild-type (Fig. 5G-I).

These data suggest that the auxin transport phenotypes of the *arr3,4,5,6,7,15* and *arr1* mutants are due at least in part to differential accumulation of PINs belonging to the PIN3, 4, 7 clade in the stem. To assess whether this is a direct effect of CK, we assessed the response of these PIN proteins to BA treatment. Inflorescence stem segments from wild-type plants were held between two agar blocks supplemented with NAA in the upper block and BA or a control solution in the lower block. After 4 h treatment, a longitudinal section was made in the basal half of the stem segment, at

or near the site of BA treatment, and imaged using confocal microscopy. The amount of PIN1-GFP on the basal plasma membrane was unchanged in mock versus BA-treated stems (Fig. 6A-C). BA treatment increased the amount of PIN3-GFP on the basal plasma membrane by ~30% ($p < 0.01$) (Fig. 6D-F), PIN4-GFP by ~20% ($p < 0.001$) (Fig. 6G-I) and PIN7-GFP by ~15% ($p < 0.01$) (Fig. 6J-L). No changes in the steady-state transcript levels of *PIN1*, *PIN3*, *PIN4* or *PIN7* were found in the basal 5 mm of equivalently treated wild-type inflorescence internodes after 4 h BA treatment (Fig. S6). When tracking individual *PIN7:PIN7-GFP*-expressing xylem parenchyma cells in a longitudinal section for 2 h, the amount of PIN7-GFP on the basal plasma membrane of NAA-treated internodes generally decreased over time, but cells treated with a combination of NAA and BA retained more PIN7-GFP signal compared to NAA alone ($p < 0.01$) (Fig. S7).

Together, the results demonstrate CK affects plasma membrane levels of PIN3, PIN4 and PIN7 proteins in inflorescence stems, and this correlates with changes in auxin transport. The effect of CK on these PINs may be post-transcriptional and the response has some specificity, since PIN1 is unaffected.

Nitrate phenocopies the effect of CK on PIN proteins in stems

Nitrate supply promotes shoot branching in Arabidopsis but the mechanisms underlying this response are complex, with multiple modes of action likely (de Jong *et al.,* 2014). The response of branching to nitrate is unlikely to involve PIN1, since steady-state PIN1-GFP levels in the stem remain the same under different nitrate regimes (de Jong *et al.,* 2014). It is well-established that CK can act as a nitrate signal (Sakakibara *et al.,* 2006) and consistent with this, we previously showed that

higher order *ipt3,5,7* and *arr3,4,5,6,7,15* mutants form similar numbers of branches under high and low nitrate conditions, suggesting CK contributes to the ability of Arabidopsis plants to modulate branching in response to nitrate supply (Müller *et al.,* 2015). The CK-responsiveness of PIN3, PIN4 and PIN7 suggests a possible route for nitrate-mediated regulation of branching via CK. To assess whether changes in nitrate status might be reflected in PIN3, PIN4 and PIN7 accumulation, *PIN3:PIN3-GFP*, *PIN4:PIN4-GFP* and *PIN7:PIN7-GFP* plants were grown under nitrate sufficient and insufficient conditions and the amount of PIN-GFP signal on the basal plasma membrane of xylem parenchyma cells quantified in basal inflorescence internodes. As for exogenous CK supply, nitrate sufficient conditions were associated with increased levels of PIN3-GFP, PIN4-GFP and PIN7-GFP on the basal plasma membrane (Fig. 7). Under low N conditions, PIN3-GFP was reduced to ~75% of the levels observed in high N plants ($p < 0.001$) (Fig. 7A), while PIN4-GFP and PIN7-GFP were reduced to approximately 85% of that in high N plants ($p < 0.001$) (Fig. 7B and C). These results are consistent with the idea that nitrate modulates shoot branching at least in part via CK effects on PIN3, PIN4 and PIN7 abundance; although, it is also possible that nitrate supply modules PIN3,4,7 accumulation via a CK-independent mechanism.

PIN3, PIN4 and PIN7 contribute to shoot branching control in *arr1*

To assess the contribution of changes in PIN3, PIN4 and PIN7 to CK-mediated branching control, we generated the *arr1 pin3 pin4 pin7* quadruple mutant (hereafter referred to as *arr1 pin3,4,7*) and analysed its branching phenotype. As the differences in branch numbers between wild type, *arr1* and *pin3,4,7* are typically small, plants were grown under short days for 4 weeks initially then shifted to long

days for 5 weeks in order to maximise branch numbers, providing sensitised conditions to assess any differences. At terminal flowering, an intermediate number of branches were formed in the *arr1 pin3,4,7* quadruple mutant (9.9) compared to the *arr1* single mutant (12.1) and the *pin3,4,7* triple mutant (8.4) (Fig. 8A-F). This reduction in branching of *arr1* in the *pin3,4,7* mutant background is consistent with the hypothesis that CK-regulated changes in PIN3, PIN4 and PIN7 contribute to the increased shoot branching phenotype of *arr1*. The *pin3,4,7* mutant exhibits twisted rosette leaves and an increased cauline branch angle phenotype (Bennett *et al.,* 2016) and in both these aspects the *arr1 pin3,4,7* quadruple mutant appeared similar to the *pin3,4,7* triple mutant (Fig. 8A-E and G).

To assess the responses of *pin3,4,7* buds to exogenous CK treatment, we used the same experimental set-up described for *arr1,* in which buds on isolated nodal stem segments were treated with apical NAA and basal BA supplied through the stem. Overall, the *pin3,4,7* triple mutant responded similarly to wild type, activating in mock and basal BA treatments and remaining inhibited for several days in the presence of apical NAA (Fig. 9A and B). As for wild type, basal BA could override the effect of apical NAA in *pin3,4,7* mutants, however, mutant buds activated significantly faster than wild type during the first four days (Fig. 9C). Together, the results suggest PIN3, PIN4 and PIN7 contribute to CK-mediated bud activation, but the phenotypic effects of *pin3,4,7* mutation suggest that CK also functions via other mechanisms.

DISCUSSION

Perturbing CK levels through exogenous application or through manipulation of endogenous levels provides clear evidence that CK can promote bud activation (Wickson and Thimann 1958; Faiss *et al.,* 1997; Chatfield *et al.,* 2000; Müller *et al.,* 2015). Elucidating the role of the known CK signalling pathway in bud activation has been less straightforward due to the large gene families involved and consequent functional redundancy. Previously, we showed that the *arr3,4,5,6,7,15* mutant has reduced branching and its buds are CK resistant – an unexpected result since type-A *ARR*s are generally considered to be negative regulators of CK signalling (Müller *et al.,* 2015). Since the type-A *ARR*s are themselves transcriptionally induced by CK as part of a negative feedback loop, loss-of-function mutations in these genes could have complex phenotypes with respect to CK response. However, our demonstration that the *arr1* mutant has a branching phenotype opposite to *arr3,4,5,6,7,15* suggests that the type-A and type-B ARRs do indeed function antagonistically in bud activation, leaving the paradox unresolved.

ARR1 and ARR3,4,5,6,7,15-independent CK signalling and shoot branching

ARR1 is a well-characterised positive regulator of CK signalling and regulates the expression of CK-responsive genes (Sakai *et al.,* 2001). Throughout our analyses of shoot branching and associated auxin transport phenotypes, *arr1* phenocopied CK treatment, whereas *arr3,4,5,6,7,15* phenocopied CK depletion, as in *ipt3* (Figs. 1, 3-6, Figs. S2 and S4). This raises the interesting prospect that the *arr* mutant phenotypes are due to feedback regulation of the pool of active CKs via synthesis or degradation, such that reduced CK signalling in *arr1* leads to an increase in the pool of active CKs, while increased CK signalling in *arr3,4,5,6,7,15* reduces the pool of

active CKs. Such feedback between hormone signalling and hormone levels is well-established for most plant hormones, including CK. For example, CK application induces expression of genes encoding CYTOKININ OXIDASE (CKX) degrading enzymes (Kiba *et al.,* 2002; Rashotte *et al.,* 2003), and this has also been observed in CK-treated buds (Müller *et al.,* 2015). Consistent with this feedback, the triple *ahk2 ahk3 cre1* CK receptor mutant has elevated levels of N^6-(Δ^2-isopentenyl)-adenine precursor and *trans*-zeatin-type CKs in young plants (Riefler *et al.,* 2006). This feedback has the potential to account for the "high CK" increased branching phenotype of the *arr1* mutant and the "low CK" reduced branching phenotype of the *arr3,4,5,6,7,15* mutant (Fig. 10).

Importantly, in addition to shoot branching, the phenotypic correlations we observe in *arr* mutants extend to auxin transport properties. CK treatment, nitrate supply, and loss of *ARR1* result in over-accumulation of PIN3, PIN4 and PIN7, whereas CK-depleting conditions such as *ipt3* mutation or nitrate starvation, and loss of the *ARR3, 4, 5, 6, 7, 15* clade result in PIN3, PIN4, and PIN7 depletion. If CK homeostasis is indeed altered in the *arr* mutants, it implies that CK can signal independently of the *ARR* genes analysed here to promote PIN3, PIN4 and PIN7 accumulation (Fig. 10). One possibility is that CK can signal entirely independently of *ARR*s via a non-canonical pathway or simply independently of *ARR1* and *ARR3, 4, 5, 6, 7, 15*, for example through a specialised type-B family member (or members) via the canonical pathway. Further work will be required to understand precisely which CK signalling components target PIN proteins in shoots. No differences were observed in PIN1 accumulation, suggesting specific auxin transporters are targeted by this signalling route.

The lack of change in *PIN* gene expression levels in type-A and type-B *arr* mutants and in wild-type plants in response to CK addition suggests *PIN* transcription is not a direct target for CK signalling in bud activation, by whatever pathway, and suggests that the effect of CK on PINs is post-transcriptional (Figs. S3 and S6). This could be a protein-level effect on PINs, similar to that established for SLs and PIN1, or it could be a transcriptional effect on PIN regulators. For example, PINOID-dependent (PID) phosphorylation can modulate the apical-basal polarity of PINs (Friml *et al.,* 2004) and *PID* expression is reduced in shoots within 2 h of CK treatment in Arabidopsis seedlings, consistent with CK promoting basal localisation of PINs (Brenner and Schmulling 2012). Such a post-transcriptional effect on PINs acting via the canonical CK signalling pathway has been established in roots. In the octuple *arr3,4,5,6,7,8,9,15* mutant, lower levels of GFP-tagged translational fusions of PIN1, 3 and 4 are observed in root tips, whereas PIN7 is reduced in the stele but increased in the root cap, and these changes do not correlate with PIN transcript abundances (Zhang *et al.,* 2011). In contrast to our results, this effect mirrors CK treatment, as expected if the type-A ARRs are acting as negative regulators of CK signalling.

The role of the auxin transport system in the regulation of shoot branching by CK

Our results show a strong correlation between CK, basal membrane abundance of PIN3, PIN4 and PIN7, bulk auxin transport and shoot branching across all our experiments. Reducing auxin transport with the pharmacological inhibitor NPA has opposite effects on branching in *arr1* and *arr3,4,5,6,7,15* (Fig. 3), suggesting a causal link between auxin transport perturbation and the *arr* mutant shoot branching

phenotypes. The *pin3,4,7* triple mutant partially suppresses the increased branching of *arr1* mutants, consistent with the idea that this phenotype is caused in part by over-accumulation of these PINs (Bennett *et al.,* 2016) (Fig. 8). One explanation for this relationship is that CK-mediated increases in PIN3, PIN4 and PIN7 accumulation increase the initial flow of auxin between the bud and the PATS, thereby supporting the establishment of canalised auxin transport between the bud and the stem and increasing the ease with which buds can activate. Consistent with this idea, polarised PIN1 protein can be observed at the bud-stem junction in pea within 24 h of CK treatment (Kalousek et al., 2010) and CK applied to axillary buds can promote the export of auxin out of the buds (Li and Bangerth 2003). This hypothesis is also consistent with the resistance of *arr1* buds to the inhibitory effects of the SL analogue GR24 (Fig. 2). SL acts in part by dampening the positive feedback in auxin transport canalisation between the bud and the stems. Increased PIN3, PIN4 and PIN7-mediated bud-stem auxin flux could counteract SL-mediated PIN1 removal by promoting additional flux-correlated PIN1 allocation. According to this model, it is the role of PIN3, PIN4 and PIN7 in cross-stem auxin flux, rather than basipetal transport down the stem that is important in CK-mediated bud activation. This is consistent with our previous analyses demonstrating that PIN3, PIN4 and PIN7 play an important role in the ability of consecutive buds on opposite sides of the stem to inhibit one another's outgrowth, while having only limited impact on the total level of shoot branching in intact plants.

Importantly, the *pin3,4,7* mutant only partially suppresses the *arr1* shoot branching phenotype and *pin3,4,7* buds respond strongly to basal BA supply in isolated nodal assays, even activating slightly earlier than wild-type buds when treated with a

combination of apical NAA and basal BA. These results demonstrate that CK can activate buds through PIN3-, PIN4- and PIN7-independent mechanisms. The mechanism(s) underlying faster *pin3,4,7* bud activation in response to apical NAA and basal BA is not known. In Arabidopsis, the ability of strigolactone to inhibit bud activity appears to depend jointly on its ability to promote accumulation of transcripts of the *BRC1* gene and to trigger endocytosis of PIN1, reducing the ability of buds to establish canalised auxin export into the stem. Our data for CK support a similar dual activity for CK, reducing *BRC1* transcript abundance and increasing PIN3,4,7 accumulation at the plasma membrane (Seale *et al.,* 2017) (Fig. 6). One highly speculative possibility is that the combination of low *BRC1* expression and reduced peripheral stem auxin in *pin3,4,7* mutants might allow for rapid early expansion of the bud.

Other targets for CK signalling in shoot branching

Our data suggest CK promotes shoot branching in part by driving plasma membrane accumulation of PIN3, PIN4 and PIN7. This would operate in parallel with the established ability of CK to regulate transcription in buds, for example by down-regulating expression of the *BRC1* bud regulatory gene (Fig. 10) (Aguilar-Martínez *et al.,* 2007; Poza-Carrion *et al.,* 2007; Braun *et al.,* 2012; Dun *et al.,* 2012; Seale *et al.,* 2017). The parallel operation of these two mechanisms makes interpretation of the *arr* mutant phenotypes complicated. For example, in the *arr1* mutant, impaired CK-induced changes in transcription should lead to reduced shoot branching. Consistent with this, the *arr1* mutant has reduced steady-state type-A *ARR* gene expression, as expected if there is reduced CK signalling via the canonical pathway (Fig. S8). At the same time, it is possible that this results in over-accumulation of CK due to impaired

feedback regulation on CK levels. This CK could signal in an *ARR1*-independent manner to promote PIN3, PIN4 and PIN7 accumulation, thereby promoting shoot branching. Thus, it is likely that the *arr1* shoot branching phenotype is a compromise between these opposing effects. Added to this, there is likely to be some redundancy in the type-B ARR family and it is possible that different family members are differentially important in regulating feedback on CK synthesis versus modulation of transcription of bud-regulating genes. Given all these considerations, there are many alternative ways to interpret our result that *arr1* mutant buds inhibited by apical NAA supply can be activated by basal BA similar to wild type, whereas *arr3,4,5,6,7,15* buds cannot (Müller *et al.,* 2015).

CONCLUSIONS

Several studies have proposed a causal link between CK and increased auxin transport as one mechanism for CK-mediated bud outgrowth (Davies *et al.,* 1966; Chatfield *et al.,* 2000; Li and Bangerth 2003). Our results support this hypothesis, and in particular we demonstrate that CK drives accumulation of PIN3, PIN4 and PIN7 on the plasma membrane, and this contributes to the branching phenotype observed in the *arr1* mutant. Interestingly, the phenotypes of type-A and type-B *arr* CK signalling mutants are the opposite of those expected given their respective negative and positive roles in CK-mediated transcriptional control in roots. This suggests strong specialisation within the *ARR* gene families or an *ARR*-independent mechanism for CK signalling in the control of shoot branching.

MATERIALS & METHODS

Plant lines

Col-0 was used as wild type for all experiments. The *arr3,4,5,6,7,15* line was published previously (Müller *et al.,* 2015). The homozygous *arr1-4* (SALK_042196) T-DNA insertion line was obtained from the Nottingham Arabidopsis Stock Centre and identified using *ARR1-4* LP (5'-GAT CAA ACC CAT TCA ATG TCG-3'), *ARR1-4* RP (5'-GAG ATG GCA TTG TCT CTG CTC-3') and LBb1.3 as per the SALK T-DNA website (www.signal.salk.edu/tdnaprimers.2.html) (Alonso *et al.,* 2003). The *PIN1:PIN1-GFP* (Benková *et al.,* 2003), *PIN3:PIN3-GFP* (Žádníková *et al.,* 2010), *PIN4:PIN4-GFP* (Bennett et al., 2016) and *PIN7:PIN7-GFP* (Blilou *et al.,* 2005) reporter lines have been described previously. All *PIN:PIN-GFP* reporter lines on the *arr3,4,5,6,7,15* mutant background were generated by crossing *arr3,4,5,6,7,15* to each of the *arr3,4,5,6,7,8,9,15 PIN-GFP* lines described previously (Zhang *et al.,* 2011) and screened for the presence of wild-type *ARR8* (F 5'-CAA ATG GCT GTT AAA ACC CAC CAA TA-3' and R 5'-CCA TTG TTA GTG TGC TAT CAC CTG AGT G-3') and *ARR9* genes (F 5'-CAG ACT CTT TAT TTC TCT TCC TC-3' and R 5'-CCC ACA TAC AAC ATC ATC ATC ATA TTC C-3'). For *arr1*, the four Col-0 *PIN:PIN-GFP* lines were crossed to *arr1-4*. Segregants were screened in the F2 and F3 generations for GFP and the correct genotype using the above gene-specific primers and *ARR3*, *-4*, *-5*, *-6*, *-7* and *-15* primers published previously (To *et al.,* 2004b; Zhang *et al.,* 2011).

Growth conditions

Seeds were stratified for 3-5 days at 4°C. Soil-grown plants were sown onto F2 soil treated with Intercept 70WG (both Levington, http://www.scottsprofessional.co.uk) or Exemptor (ICL, http://icl-sf.com/uk-en) in P24 or P40 trays in controlled environment rooms under long-day (16 h light/ 8 h dark) or short-day (8 h light/16 h dark) photoperiods. For plants grown under sterile conditions, seeds were vapour-sterilised with 100 mL 10% (w/v) chlorine bleach and 3 mL 10.2 M HCl for 4 h and sown onto solidified ATS medium (containing 0.8% agar) (Wilson *et al.,* 1990). Soil and sterile-grown plants were subject to an average light intensity of 170 or 100 µmol m^{-2} sec^{-1}, respectively, and an average temperature range of 17–21°C.

Branch counts

Primary rosette and cauline branches ≥1 cm were counted on intact plants at or near terminal flowering. Decapitation assays were performed as per Greb *et al*. (2003).

Hormone and NPA treatments

For testing bud responses to NAA, BA and GR24, plants were grown under sterile conditions and one-node assays performed as previously described (Chatfield *et al.,* 2000; Müller *et al.,* 2015). For treating whole plants with NPA or GR24, plants were grown for 6 weeks under sterile conditions on solidified ATS in glass jars as described previously (Bennett *et al.,* 2006; Crawford *et al.,* 2010). For NAA and BA treatment of stems, 2 cm segments from the basal inflorescence internode were collected from soil-grown plants. Similar to the one-node assay system, segments were placed vertically into split plates prepared with 1 µM NAA in the upper apical portion and either mock (DMSO) or 1 µM BA in the lower basal portion, or the apical portion. Plates were prepared by cutting a 1 cm trough through the middle of square

10 cm plates containing 50 mL solidified ATS without sucrose. Hormone or mock solutions were pipetted into the upper or lower half (25 µL of 1000X stocks). Plates were placed under standard light conditions for sterile-grown plants.

Reverse transcription quantitative PCR

For analysis of *PIN1*, *PIN3*, *PIN4* and *PIN7* gene expression levels in the *arr1* and *arr3,4,5,6,7,15* mutants, seeds were sown in glass jars on solidified ATS as described above for whole-plant NPA and GR24 treatments. Plants were grown for 6 weeks and the uppermost inflorescence internodes (i.e. the inflorescence stem between the uppermost two cauline nodes) harvested onto liquid nitrogen. Three biological replicates each containing 10-15 internodes were collected. For NAA and BA treatments, 2 cm segments from the basal inflorescence internodes were collected from 6 week old soil-grown plants and placed vertically into plates containing apical NAA with or without basal BA, prepared as above. Treatments were left for 4 h and the basal 5 mm of the 2 cm segments were harvested into three biological replicates of 6-7 segments each on liquid nitrogen. RNA extractions, cDNA synthesis and quantification of transcript levels were carried out as described previously (Müller *et al.,* 2015) using 650 or 500 ng total RNA for the *arr* or BA response analyses, respectively. Sequences of primers used are as follows: *PIN1* F 5'-CAG TCT TGG GTT GTT CAT GGC-3', *PIN1* R 5'-ATC TCA TAG CCG CCG CAA AA-3', *PIN3* F 5'-CCA TGG CGG TTA GGT TCC TT-3', *PIN3* R 5'-ATG CGG CCT GAA CTA TAG CG-3', *PIN4* F 5'-AAT GCT AGA GGT GGT GGT GAT G-3', *PIN4* R 5'-TAG CTC CGC CGT GGA ATT AG-3', *PIN7* F 5'-GGT GAA AAC AAA GCT GGT CCG-3' and *PIN7* R 5'-CCG AAG CTT GTG TAG TCC GT-3'. For Fig. S8, *ARR1* F 5'-TAC GAA GTA ACG AAA TGC AAC AGA-3', *ARR1* R 5'-GAA ACC GTC CAT

GTC AGG CA-3', and previously published primer sequences for *ARR4*, *5*, *6*, *7* and *15* were used (Müller *et al.,* 2015).

Microscopy

For *PIN1:PIN1-GFP* and *PIN3:PIN3-GFP*, which exhibit relatively stable levels of expression in the stem throughout development, basal inflorescence internodes from ~6 week old soil-grown plants were collected for imaging. For *PIN4:PIN4-GFP* and *PIN7:PIN7-GFP*, which exhibit a reduction in stem expression during development, inflorescence internodes were taken from 4–5-week-old soil-grown plants when the inflorescence was approximately 5-15 cm high. Between treatments, individual plants were stage-matched so that the same internodes from two plants with inflorescence heights within 1 cm of each other were compared. Internodes were hand-sectioned longitudinally through vascular bundles using a razor blade under a dissecting microscope, or transversely in 2 mm segments, then secured to a petri dish with micropore tape or embedded in solidified ATS and covered in water. Confocal microscopy was performed using a Zeiss LSM700 imaging system with 20X or 10X water immersion lenses. For longitudinal sections, xylem parenchyma tissues were located by focussing on the helical pattern of xylem cell wall lignin under transmitted light. Excitation was performed using 488 nm (3-6% laser power) and 639 nm (2% laser power) lasers. Images were acquired using SP 555 and LP640 emission filters for GFP and chloroplast autofluorescence, respectively. The same detection settings were used within an experiment. For longitudinal sections, GFP fluorescence intensities were quantified by manually tracing around the basal plasma membrane of a non-saturated cell using Zeiss ZEN 2012 software. At least five cells each from 8-10 individual plants were analysed per treatment and repeated

at least once. For transverse sections, Z-stacks were acquired using a 3-5 μm step size. Maximum projections generated using ImageJ software and GFP fluorescence (as arbitrary units per pixel) quantified by manually tracing around vascular bundles. Five vascular bundles were analysed from at least five individual plants and repeated at least once. For representative images, projections were made using LSM Image Browser software version 4.2.0.121 and processed in Adobe Photoshop.

Auxin transport assays

Auxin transport assays were performed as per (Bennett *et al.,* 2016).

Branch angle measurements

Inflorescence stems bearing two branches from mature plants were trimmed, laid flat and photographed. The angle between the point of emergence and the inflorescence stem was measured using ImageJ software.

Statistical analyses

Statistical analyses were performed using SPSS Statistics version 22.

ACCESSION NUMBERS

Sequence data form this article can be found on The Arabidopsis Information Resource (TAIR; www.arabidopsis.org) under accession numbers AT3G16857 (ARR1), AT1G59940 (ARR3), AT1G10470 (ARR4), AT3G48100 (ARR5), AT5G62920 (ARR6), AT1G19050 (ARR7), AT1G74890 (ARR15), AT3G63110 (IPT3), AT1G73590 (PIN1), AT1G70940 (PIN3), AT2G01420 (PIN4) and AT1G23080 (PIN7).

SUPPLEMENTAL FIGURES

Figure S1. GR24 dose response of wild-type and *arr1*.

Figure S2. *ipt3* has reduced stem auxin transport.

Figure S3. *PIN* gene expression in wild-type, *arr1* and *arr3,4,5,6,7,15* mutants.

Figure S4. PIN7-GFP is reduced in *ipt3* inflorescence stems.

Figure S5. PIN7-GFP expression in *arr1* inflorescence stems over time.

Figure S6. *PIN* gene expression is unchanged in inflorescence stems after 4 h BA treatment.

Figure S7. BA promotes accumulation of PIN7:PIN7-GFP on the basal plasma membrane of xylem parenchyma cells within 2 h.

Figure S8. Expression of *ARR* genes in *arr* mutants.

ACKNOWLEDGEMENTS

We thank Joseph Kieber for kindly supplying the *arr3,4,5,6,7,8,9,15* PIN-GFP reporter lines, Ruth Stephens for excellent technical assistance and Tom Bennett and Martin van Rongen for helpful advice and discussions.

FIGURE LEGENDS

Figure 1. An *ARR1* mutation confers increased shoot branching. A) Rosette branches formed 10 days after primary shoot decapitation in plants grown in short days for 4 weeks and long days for ~3 weeks, as per Greb *et al*. (2006) (*n* = 38-40). B) Total branches (rosette and cauline) formed in Col-0 and *arr1-4* plants grown in long days for ~6 weeks (*n* = 30-31). C-E) Shoot branching phenotypes of Col-0 and *arr1-4* plants grown in long days for ~7 weeks. A close-up view of the rosettes in C are shown in D (Col-0) and E (*arr1-4*). Bars indicate S.E.M., statistical comparisons shown are between mutant and wild type (Mann-Whitney test, ** = $p < 0.01$, *** = < 0.001).

Figure 2. *arr1* buds have wild-type responses to auxin and cytokinin but are resistant to strigolactone. Wild type (A and C) or *arr1* (B and D) isolated nodal segments bearing one bud were treated for 8 days with (A and B) mock, 1 µM NAA (apical) 1 µM BA (basal) or combined 1 µM NAA (apical) and 1 µM BA (basal) (*n* = 18-20 per treatment), or (C and D) 0.5 µM NAA (apical) or combined 0.5 µM NAA (apical) and 5 µM GR24 (*n* = 18-20). Bars indicate S.E.M. Statistical comparisons shown were made between NAA and NAA + GR24 treated buds at each time point (Student's *t*-test, * = $p < 0.05$, ** = $p < 0.01$).

Figure 3. Type-A and type-B *arr* mutant branching phenotypes are associated with altered auxin transport. A) Amount of apically applied ^{14}C-IAA (CPM; counts per minute) transported to the basal end of inflorescence stem internodes from ~6 week old wild-type, *arr1* and *arr3,4,5,6,7,15* plants in 6 hours (*n* = 24-32). Different letters

denote significant difference (ANOVA, Tukey-b post-hoc test, $p < 0.05$). B) NPA dose response of wild-type and *arr1* plants grown for 6 weeks on different concentrations of NPA under sterile conditions (n = 18-42). C) NPA dose response of wild-type and *arr3,4,5,6,7,15* plants grown for 6 weeks on different concentrations of NPA under sterile conditions (n = 13-24). For A-C bars indicate S.E.M. For B and C, letters denote significant difference within a genotype (Kruskal-Wallis H test, $p < 0.05$).

Figure 4. PIN3-GFP and PIN7-GFP accumulation is attenuated in *arr3,4,5,6,7,15* inflorescence stems. Representative accumulation patterns of PIN1-GFP (A and B), PIN3-GFP (D and E) and PIN7-GFP (G and H) in basal inflorescence internodes of Col-0 (A, D and G) and *arr3,4,5,6,7,15* (B, E and H) plants, imaged at ~5-6 weeks of age using confocal microscopy. For confocal images, green shows PIN-GFP signal and magenta shows chloroplast autofluorescence. Scale bars represent 10 μm (A, B, D and E) or 200 μm (G and H). For *PIN1:PIN1-GFP* and *PIN3:PIN3-GFP*, plants were sectioned longitudinally and the amount of GFP signal on the basal plasma membrane was quantified in the xylem parenchyma using at least five cells each from eight independent plants (C and F) (n = 40). For *PIN7:PIN7-GFP*, plants were sectioned transversely (~2 mm thickness) and the amount of GFP signal was quantified in at least five vascular bundles from five independent plants with inflorescence stems stage-matched at 24-26 cm in height (I) (n = 25). Bars indicate S.E.M., statistical comparisons shown were made between mutant and wild type (Student's t-test, $p < 0.001$).

Figure 5. PIN3-GFP and PIN7-GFP accumulation is elevated in *arr1* inflorescence stems. Representative accumulation patterns of PIN1-GFP (A and B), PIN3-GFP (D

and E) and PIN7-GFP (G and H) in basal inflorescence internodes of 4–7-week-old Col-0 (A, D and G) and *arr1* (B, E and H) plants, sectioned longitudinally and imaged using confocal microscopy. Green shows PIN-GFP signal and magenta shows chloroplast autofluorescence. Scale bars represent 10 μm. The amount of GFP signal on the basal plasma membrane was quantified in the xylem parenchyma using at least five cells each from eight independent plants (C, F and I) (n = 40). For *PIN1:PIN1-GFP* and *PIN3:PIN3-GFP*, plants were analysed at 6-7 weeks of age. For *PIN7:PIN7-GFP*, plants were stage-matched by comparing plants with inflorescence stems 18-20 cm in height. Bars indicate S.E.M., statistical comparisons shown were made between mutant and wild type (Student's *t*-test, * = $p < 0.05$, ** = $p < 0.01$).

Figure 6. Cytokinin promotes the accumulation of PIN3-GFP, PIN4-GFP and PIN7-GFP on the basal plasma membrane of xylem parenchyma cells in inflorescence stems. Vertically held basal inflorescence internode segments (~2 cm) from *PIN1:PIN1-GFP* (A-C), *PIN3:PIN3-GFP* (D-F), *PIN4:PIN4-GFP* (G-I) and *PIN7:PIN7-GFP* (J-L) plants (all Col-0 background), were treated apically with 1 μM NAA and basally with either 0.1% DMSO control ("Mock") or 1 μM BA ("+ BA"). After 4 hours, stem segments were sectioned longitudinally at their basal ends and imaged using confocal microscopy. The amount of GFP signal on the basal plasma membrane of xylem parenchyma cells was quantified in five cells each from at least seven independent plants for *PIN1:PIN1-GFP* (A), ten independent plants for *PIN3:PIN3-GFP* (D) and *PIN4:PIN4-GFP* (G), or eleven independent plants for *PIN7:PIN7-GFP* (J). Bars indicate S.E.M., statistical comparisons shown were made between mock and BA treated stems (Student's *t*-test, * = $p < 0.05$, ** = $p < 0.01$). Representative confocal images used for GFP quantifications are shown for mock (B, E, H and K)

and BA (C, F, I and L) treated stems. Green shows PIN-GFP signal and magenta shows chloroplast autofluorescence. *PIN1:PIN1-GFP* and *PIN3:PIN3-GFP* plants were analysed at 5-6 weeks of age. *PIN4:PIN4-GFP* and *PIN7:PIN7-GFP* plants were analysed at 4-5 weeks of age and stage-matched across treatments according to inflorescence height. Scale bars represent 10 μm.

Figure 7. Growth on low nitrate (N) conditions reduces PIN-GFP accumulation. *PIN3:PIN3-GFP* (A), *PIN4:PIN4-GFP* (B) and *PIN7:PIN7-GFP* (C) plants (all Col-0 background) were grown on a sand and terragreen mix supplemented with ATS medium containing 9.0 mM NO_3 (high N) or 1.8 mM NO_3 (low N). Basal inflorescence internodes were sectioned longitudinally and imaged at 4-6 weeks of age using confocal microscopy. *PIN7:PIN7-GFP* plants were stage matched based on inflorescence heights across N treatments. The amount of GFP signal on the basal plasma membrane was quantified in the xylem parenchyma using five cells each from eight independent plants for (C) (n = 40). Bars indicate S.E.M., statistical comparisons shown were made between high and low N treated plants (Student's t-test, $p < 0.001$).

Figure 8. Interactions between *arr1* and *pin3,4,7* in shoot branching control. A-E) Shoot phenotypes of ~6 week old Col-0, *arr1*, *pin3,4,7* and *arr1 pin3,4,7* plants grown under long days. A close-up view of the rosettes in A are shown in B (Col-0), C (*arr1*), D (*pin3,4,7*) and E (*arr1 pin3,4,7*). F) Total number of branches formed at terminal flowering on ~9 week old wild-type, *arr1*, *pin3,4,7* and *arr1 pin3,4,7* plants grown under short days for 4 weeks then long days for 5 weeks (n = 16-47). Bars indicate S.E.M. Letters denote significant difference between genotypes (Kruskal-

Wallis H test, $p < 0.05$). G) Angle between emergence point of branches on the primary inflorescence in wild-type, *arr1*, *pin3,4,7* and *arr1 pin3,4,7* plants at ~6 weeks of age. Two cauline branches were analysed per plant from at least 13 independent plants (n = 26-46). Bars indicate S.E.M. Letters denote significant difference (ANOVA, Tukey-b post-hoc test, $p < 0.05$).

Figure 9. *pin3,4,7* exhibits altered bud activation in response to BA. Bud length of wild type (Col-0) (A) and *pin3,4,7* (B) isolated nodal segments treated for 8 days with mock, 1 µM NAA (apical), 1 µM BA (basal) or combined 1 µM NAA (apical) and 1 µM BA (basal) (n = 19-20 per treatment). (C) Close-up of days 0-4 for wild-type and *pin3,4,7* buds treated with combined apical NAA and basal BA. Bars indicate S.E.M. Asterisks denote statistically significant difference between treatments (Student's *t*-test, * = $p < 0.05$, *** = $p < 0.001$).

Figure 10. Proposed model for CK signalling in bud outgrowth regulation. Canonical CK signalling via the type-B ARR1 results in feedback-mediated down-regulation of CK levels as part of signal perception. Members of the type-A ARR family are transcriptionally induced by ARR1 and/or other type-B family members, and dampen type-B-mediated signalling, including the feedback-mediated down-regulation of CK levels. Basal plasma-membrane accumulation of PIN3, PIN4 and PIN7 in xylem parenchyma cells in the main stem is enhanced by CK by an unknown mechanism. In parallel, expression of other bud regulatory genes such as *BRC1* may be targeted by the canonical CK signalling pathway.

LITERATURE CITED

Aguilar-Martínez, J.A., Poza-Carrión, C. and Cubas, P. (2007) *Arabidopsis BRANCHED1* acts as an integrator of branching signals within axillary buds. *Plant Cell*, 19, 458-472.

Alonso, J.M., Stepanova, A.N., Leisse, T.J., Kim, C.J., Chen, H., Shinn, P., Stevenson, D.K., Zimmerman, J., Barajas, P., Cheuk, R., Gadrinab, C., Heller, C., Jeske, A., Koesema, E., Meyers, C.C., Parker, H., Prednis, L., Ansari, Y., Choy, N., Deen, H., Geralt, M., Hazari, N., Hom, E., Karnes, M., Mulholland, C., Ndubaku, R., Schmidt, I., Guzman, P., Aguilar-Henonin, L., Schmid, M., Weigel, D., Carter, D.E., Marchand, T., Risseeuw, E., Brogden, D., Zeko, A., Crosby, W.L., Berry, C.C. and Ecker, J.R. (2003) Genome-wide insertional mutagenesis of Arabidopsis thaliana. *Science*, 301, 653-657.

Bainbridge, K., Sorefan, K., Ward, S. and Leyser, O. (2005) Hormonally controlled expression of the Arabidopsis *MAX4* shoot branching regulatory gene. *Plant J.*, 44, 569-580.

Bangerth, F. (1994) Response of cytokinin concentration in the xylem exudate of bean (*Phaseolus vulgaris* L.) plants to decapitation and auxin treatment, and relationship to apical dominance. *Planta*, 194, 4.

Benková, E., Michniewicz, M., Sauer, M., Teichmann, T., Seifertová, D., Jürgens, G. and Friml, J. (2003) Local, efflux-dependent auxin gradients as a common module for plant organ formation. *Cell*, 115, 591-602.

Bennett, T., Sieberer, T., Willett, B., Booker, J., Luschnig, C. and Leyser, O. (2006) The *Arabidopsis MAX* pathway controls shoot branching by regulating auxin transport. *Curr. Biol.*, 16, 553-563.

Bennett, T., Hines, G., van Rongen, M., Waldie, T., Sawchuk, M.G., Scarpella, E., Ljung, K. and Leyser, O. (2016) Connective Auxin Transport in the Shoot Facilitates Communication between Shoot Apices. *PLoS Biol*, 14, e1002446.

Blilou, I., Xu, J., Wildwater, M., Willemsen, V., Paponov, I., Friml, J., Heidstra, R., Aida, M., Palme, K. and Scheres, B. (2005) The PIN auxin efflux facilitator network controls growth and patterning in *Arabidopsis* roots. *Nature*, 433, 39-44.

Booker, J., Chatfield, S. and Leyser, O. (2003) Auxin acts in xylem-associated or medullary cells to mediate apical dominance. *Plant Cell*, 15, 495-507.

Braun, N., de Saint Germain, A., Pillot, J.P., Boutet-Mercey, S., Dalmais, M., Antoniadi, I., Li, X., Maia-Grondard, A., Le Signor, C., Bouteiller, N., Luo, D., Bendahmane, A., Turnbull, C. and Rameau, C. (2012) The pea TCP transcription factor PsBRC1 acts downstream of strigolactones to control shoot branching. *Plant Physiol.*, 158, 225-238.

Brenner, W.G. and Schmulling, T. (2012) Transcript profiling of cytokinin action in Arabidopsis roots and shoots discovers largely similar but also organ-specific responses. *BMC Plant Biol*, 12, 112.

Chatfield, S.P., Stirnberg, P., Forde, B.G. and Leyser, O. (2000) The hormonal regulation of axillary bud growth in *Arabidopsis*. *Plant J.*, 24, 159-169.

Crawford, S., Shinohara, N., Sieberer, T., Williamson, L., George, G., Hepworth, J., Müller, D., Domagalska, M.A. and Leyser, O. (2010) Strigolactones enhance competition between shoot branches by dampening auxin transport. *Development*, 137, 2905-2913.

Davies, C.R., Seth, A.K. and Wareing, P.F. (1966) Auxin and kinetin interaction in apical dominance. *Science*, 151, 468-469.

de Jong, M., George, G., Ongaro, V., Williamson, L., Willetts, B., Ljung, K., McCulloch, H. and Leyser, O. (2014) Auxin and strigolactone signaling are required for modulation of Arabidopsis shoot branching by nitrogen supply. *Plant Physiol*, 166, 384-395.

Domagalska, M.A. and Leyser, O. (2011) Signal integration in the control of shoot branching. *Nat Rev Mol Cell Biol*, 12, 211-221.

Dun, E.A., de Saint Germain, A., Rameau, C. and Beveridge, C.A. (2012) Antagonistic action of strigolactone and cytokinin in bud outgrowth control. *Plant Physiol.*, 158, 487-498.

Faiss, M., Zalubilova, J., Strnad, M. and Schmulling, T. (1997) Conditional transgenic expression of the ipt gene indicates a function for cytokinins in paracrine signaling in whole tobacco plants. *Plant J*, 12, 401-415.

Foo, E., Turnbull, C.G. and Beveridge, C.A. (2001) Long-distance signaling and the control of branching in the rms1 mutant of pea. *Plant Physiol*, 126, 203-209.

Foo, E., Bullier, E., Goussot, M., Foucher, F., Rameau, C. and Beveridge, C.A. (2005) The branching gene *RAMOSUS1* mediates interactions among two novel signals and auxin in pea. *Plant Cell*, 17, 464-474.

Friml, J., Yang, X., Michniewicz, M., Weijers, D., Quint, A., Tietz, O., Benjamins, R., Ouwerkerk, P.B., Ljung, K., Sandberg, G., Hooykaas, P.J., Palme, K. and Offringa, R. (2004) A PINOID-dependent binary switch in apical-basal PIN polar targeting directs auxin efflux. *Science*, 306, 862-865.

Geldner, N., Anders, N., Wolters, H., Keicher, J., Kornberger, W., Muller, P., Delbarre, A., Ueda, T., Nakano, A. and Jurgens, G. (2003) The Arabidopsis GNOM ARF-GEF mediates endosomal recycling, auxin transport, and auxin-dependent plant growth. *Cell*, 112, 219-230.

Greb, T., Clarenz, O., Schäfer, E., Müller, D., Herrero, R., Schmitz, G. and Theres, K. (2003) Molecular analysis of the *LATERAL SUPPRESSOR* gene in *Arabidopsis* reveals a conserved control mechanism for axillary meristem formation. *Genes Dev.*, 17, 1175-1187.

Hall, S.M. and Hillman, J.R. (1975) Correlative inhibition of lateral bud growth in *Phaseolus vulgaris* L.: timing of bud growth following decapitation. *Planta*, 123, 137-143.

Hayward, A., Stirnberg, P., Beveridge, C. and Leyser, O. (2009) Interactions between auxin and strigolactone in shoot branching control. *Plant Physiol.*, 151, 400-412.

Johnson, X., Brcich, T., Dun, E.A., Goussot, M., Haurogné, K., Beveridge, C.A. and Rameau, C. (2006) Branching genes are conserved across species. Genes controlling a novel signal in pea are coregulated by other long-distance signals. *Plant Physiol.*, 142, 1014-1026.

Kalousek, P., Buchtová, D., Balla, J., Reinöhl, V. and Procházka, S. (2010) Cytokinins and polar transport of auxin in axillary pea buds. *Acta Univ. Agric. Silvic. Mendel. Brun.*, 58, 10.

Kiba, T., Yamada, H. and Mizuno, T. (2002) Characterization of the ARR15 and ARR16 response regulators with special reference to the cytokinin signaling pathway mediated by the AHK4 histidine kinase in roots of Arabidopsis thaliana. *Plant Cell Physiol*, 43, 1059-1066.

Li, C. and Bangerth, F. (2003) Stimulatory effect of cytokinins and interaction with IAA on the release of lateral buds of pea plants from apical dominance. *J Plant Physiol*, 160, 1059-1063.

Ljung, K., Bhalerao, R.P. and Sandberg, G. (2001) Sites and homeostatic control of auxin biosynthesis in *Arabidopsis* during vegetative growth. *Plant J.*, 28, 465-474.

Miyawaki, K., Tarkowski, P., Matsumoto-Kitano, M., Kato, T., Sato, S., Tarkowska, D., Tabata, S., Sandberg, G. and Kakimoto, T. (2006) Roles of *Arabidopsis* ATP/ADP isopentenyltransferases and tRNA isopentenyltransferases in cytokinin biosynthesis. *Proc. Natl Acad. Sci. U.S.A.*, 103, 16598-16603.

Morris, D.A. (1977) Transport of exogenous auxin in 2-branched dwarf pea seedlings (*Pisum sativum* L.) - some implications for polarity and apical dominance. *Planta*, 136, 91-96.

Müller, D., Waldie, T., Miyawaki, K., To, J.P., Melnyk, C.W., Kieber, J.J., Kakimoto, T. and Leyser, O. (2015) Cytokinin is required for escape but not release from auxin mediated apical dominance. *Plant J*, 82, 874-886.

Poza-Carrion, C., Aguilar-Martinez, J.A. and Cubas, P. (2007) Role of TCP Gene BRANCHED1 in the Control of Shoot Branching in Arabidopsis. *Plant Signal Behav*, 2, 551-552.

Prusinkiewicz, P., Crawford, S., Smith, R.S., Ljung, K., Bennett, T., Ongaro, V. and Leyser, O. (2009) Control of bud activation by an auxin transport switch. *Proc. Natl Acad. Sci. U.S.A.*, 106, 17431-17436.

Rashotte, A.M., Carson, S.D., To, J.P. and Kieber, J.J. (2003) Expression profiling of cytokinin action in Arabidopsis. *Plant Physiol*, 132, 1998-2011.

Riefler, M., Novak, O., Strnad, M. and Schmulling, T. (2006) Arabidopsis cytokinin receptor mutants reveal functions in shoot growth, leaf senescence, seed size, germination, root development, and cytokinin metabolism. *Plant Cell*, 18, 40-54.

Ruegger, M., Dewey, E., Hobbie, L., Brown, D., Bernasconi, P., Turner, J., Muday, G. and Estelle, M. (1997) Reduced naphthylphthalamic acid binding in the tir3 mutant of Arabidopsis is associated with a reduction in polar auxin transport and diverse morphological defects. *Plant Cell*, 9, 745-757.

Sachs, T. (1981) The control of the patterned differentiation of vascular tissues. *Adv. Bot. Res.*, 9, 151-262.

Sakai, H., Honma, T., Aoyama, T., Sato, S., Kato, T., Tabata, S. and Oka, A. (2001) ARR1, a transcription factor for genes immediately responsive to cytokinins. *Science*, 294, 1519-1521.

Sakakibara, H., Takei, K. and Hirose, N. (2006) Interactions between nitrogen and cytokinin in the regulation of metabolism and development. *Trends Plant Sci*, 11, 440-448.

Schaller, G.E., Bishopp, A. and Kieber, J.J. (2015) The yin-yang of hormones: cytokinin and auxin interactions in plant development. *Plant Cell*, 27, 44-63.

Seale, M., Bennett, T. and Leyser, O. (2017) BRC1 expression regulates bud activation potential but is not necessary or sufficient for bud growth inhibition in Arabidopsis. *Development*, 144, 1661-1673.

Shinohara, N., Taylor, C. and Leyser, O. (2013) Strigolactone can promote or inhibit shoot branching by triggering rapid depletion of the auxin efflux protein PIN1 from the plasma membrane. *PLoS Biol.*, 11, e1001474.

Tanaka, M., Takei, K., Kojima, M., Sakakibara, H. and Mori, H. (2006) Auxin controls local cytokinin biosynthesis in the nodal stem in apical dominance. *Plant J*, 45, 1028-1036.

Teichmann, T. and Muhr, M. (2015) Shaping plant architecture. *Front Plant Sci*, 6, 233.

Thimann, K.V. and Skoog, F. (1933) Studies on the growth hormone of plants: III. The inhibiting action of the growth substance on bud development. *Proc. Natl Acad. Sci. U.S.A.*, 19, 714-716.

To, J.P., Haberer, G., Ferreira, F.J., Deruere, J., Mason, M.G., Schaller, G.E., Alonso, J.M., Ecker, J.R. and Kieber, J.J. (2004a) Type-A Arabidopsis response regulators are partially redundant negative regulators of cytokinin signaling. *Plant Cell*, 16, 658-671.

To, J.P., Haberer, G., Ferreira, F.J., Deruère, J., Mason, M.G., Schaller, G.E., Alonso, J.M., Ecker, J.R. and Kieber, J.J. (2004b) Type-A *Arabidopsis* response regulators are partially redundant negative regulators of cytokinin signaling. *Plant Cell*, 16, 658-671.

Wickson, M. and Thimann, K.V. (1958) The antagonism of auxin and kinetin in apical dominance. *Physiol. Plantarum*, 11, 62-74.

Wilson, A.K., Pickett, F.B., Turner, J.C. and Estelle, M. (1990) A dominant mutation in *Arabidopsis* confers resistance to auxin, ethylene and abscisic acid. *Mol. Gen. Genet.*, 222, 377-383.

Žádníková, P., Petrášek, J., Marhavý, P., Raz, V., Vandenbussche, F., Ding, Z., Schwarzerová, K., Morita, M.T., Tasaka, M., Hejátko, J., Van Der Straeten, D., Friml, J. and Benková, E. (2010) Role of PIN-mediated auxin efflux in apical hook development of *Arabidopsis thaliana*. *Development*, 137, 607-617.

Zhang, W., To, J.P., Cheng, C.Y., Schaller, G.E. and Kieber, J.J. (2011) Type-A response regulators are required for proper root apical meristem function through post-transcriptional regulation of PIN auxin efflux carriers. *Plant J.*, 68, 1-10.

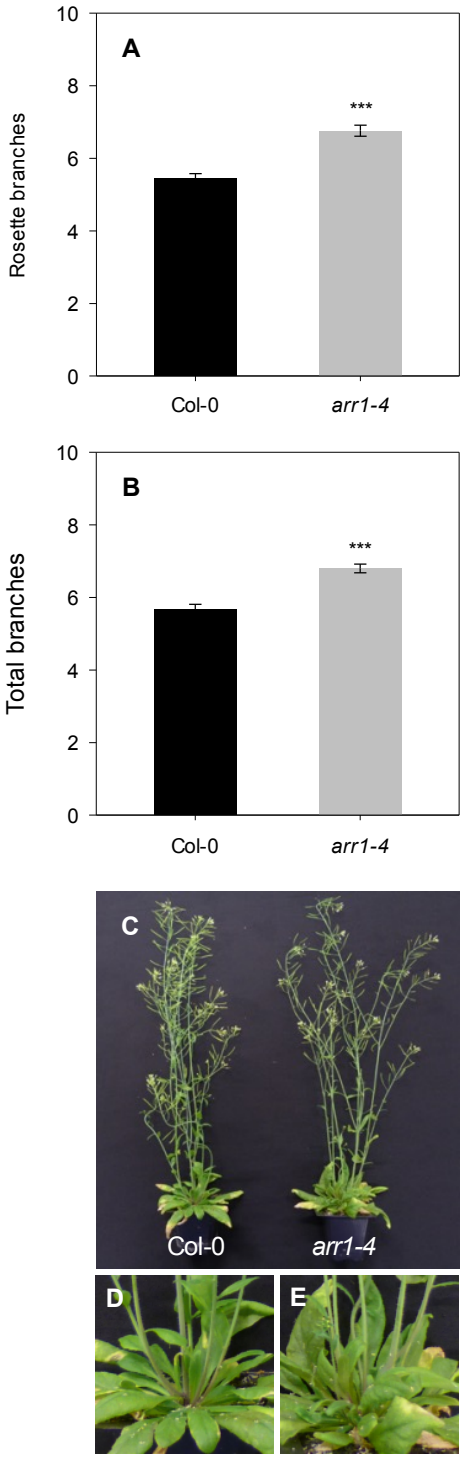

Figure 1. An *ARR1* mutation confers increased shoot branching. A) Rosette branches formed 10 days after primary shoot decapitation in plants grown in short days for 4 weeks and long days for ~3 weeks, as per Greb *et al*. (2006) (*n* = 38-40).

B) Total branches (rosette and cauline) formed in Col-0 and *arr1-4* plants grown in long days for ~6 weeks (*n* = 30-31). C-E) Shoot branching phenotypes of Col-0 and *arr1-4* plants grown in long days for ~7 weeks. A close-up view of the rosettes in C are shown in D (Col-0) and E (*arr1-4*). Bars indicate S.E.M., statistical comparisons shown are between mutant and wild-type (Mann-Whitney test, ** = $p < 0.01$, *** = < 0.001).

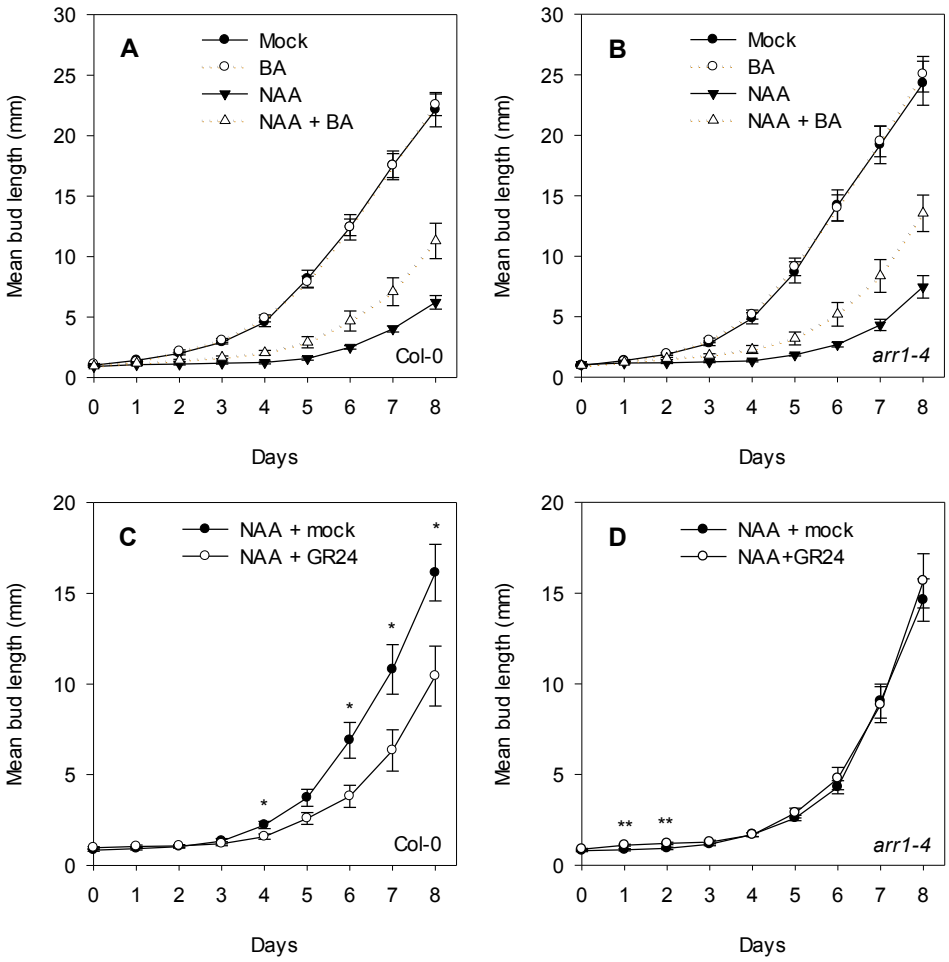

Figure 2. *arr1* buds have wild-type responses to auxin and cytokinin but are resistant to strigolactone. Wild-type (A and C) or *arr1* (B and D) isolated nodal segments bearing one bud were treated for 8 days with (A and B) mock, 1 µM NAA (apical) 1 µM BA (basal) or combined 1 µM NAA (apical) and 1 µM BA (basal) (*n* = 18-20 per treatment), or (C and D) 0.5 µM NAA (apical) or combined 0.5 µM NAA (apical) and 5 µM GR24 (*n* = 18-20). Bars indicate S.E.M. Statistical comparisons shown were made between NAA and NAA + GR24 treated buds at each time point (Student's *t*-test, * = $p < 0.05$, ** = $p < 0.01$).

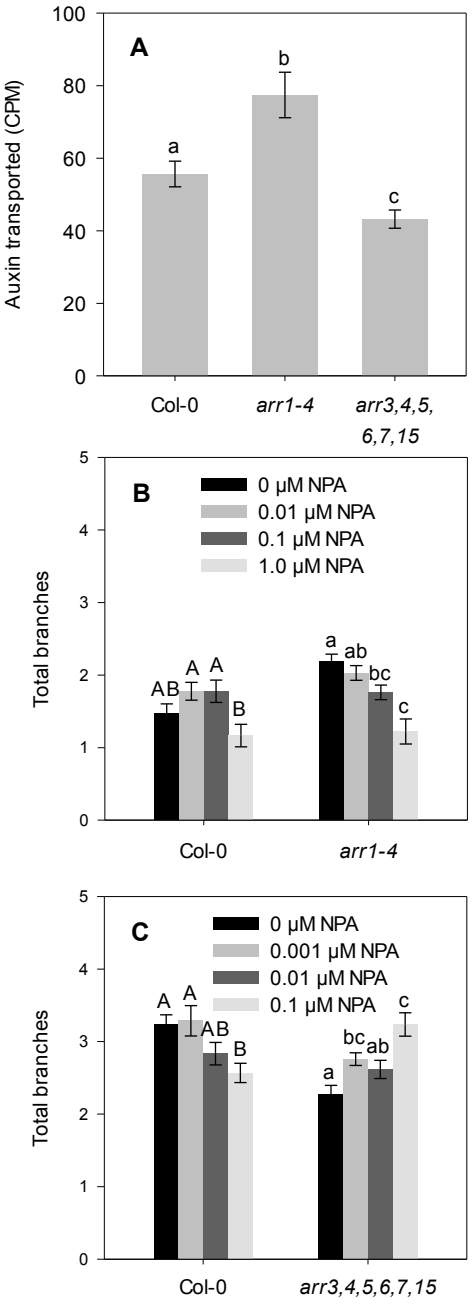

Figure 3. Type-A and type-B *arr* mutant branching phenotypes are associated with altered auxin transport. A) Amount of apically applied ^{14}C-IAA (counts per minute) transported to the basal end of inflorescence stem internodes from ~6 week old wild-type, *arr1* and *arr3,4,5,6,7,15* plants in 6 hours (n = 24-32). Different letters denote significant difference (ANOVA, Tukey-b post-hoc test, $p < 0.05$). B) NPA dose

response of wild-type and *arr1* plants grown for 6 weeks on different concentrations of NPA under sterile conditions (n = 18-42). C) NPA dose response of wild-type and *arr3,4,5,6,7,15* plants grown for 6 weeks on different concentrations of NPA under sterile conditions (n = 13-24). For A-C bars indicate S.E.M. For B and C, letters denote significant difference within a genotype (Kruskal-Wallis H test, $p < 0.05$).

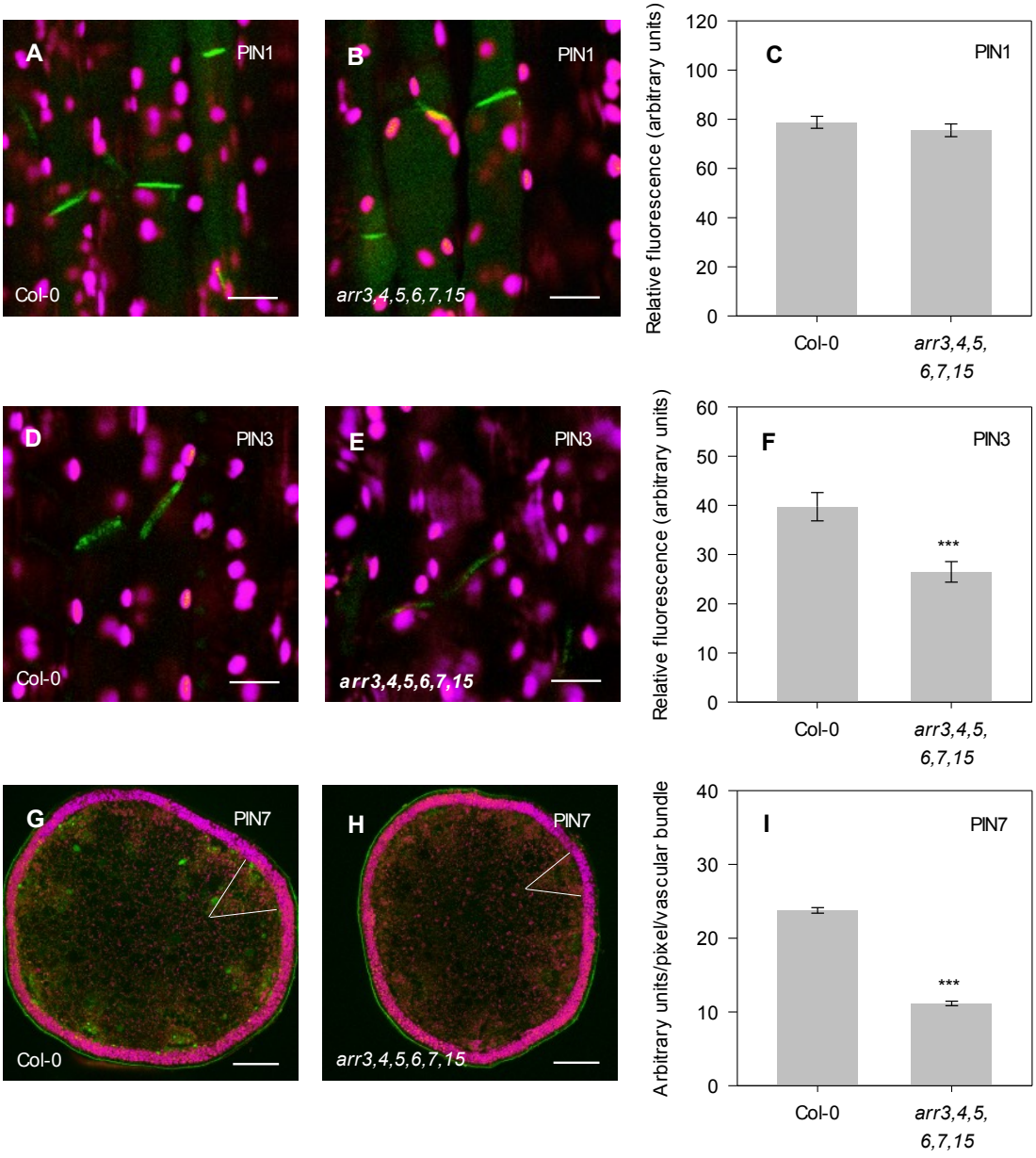

Figure 4. PIN3:PIN3-GFP and PIN7:PIN7-GFP expression is attenuated in *arr3,4,5,6,7,15* inflorescence stems. Representative expression patterns of PIN1:PIN1-GFP (A and B), PIN3:PIN3-GFP (D and E) and PIN7:PIN7-GFP (G and H) in basal inflorescence internodes of Col-0 (A, D and G) and *arr3,4,5,6,7,15* (B, E and H) plants, imaged at ~5-6 weeks of age using confocal microscopy. For confocal images, green shows PIN-GFP signal and magenta shows chloroplast

autofluorescence. Scale bars represent 10 μm (A, B, D and E) or 200 μm (G and H). For PIN1:PIN1-GFP and PIN3:PIN3-GFP, plants were sectioned longitudinally and the amount of GFP signal on the basal plasma membrane was quantified in the xylem parenchyma using at least five cells each from eight independent plants (C and F) (n = 40). For PIN7:PIN7-GFP, plants were sectioned transversely (~2 mm thickness) and the amount of GFP signal was quantified in at least five vascular bundles from five independent plants with inflorescence stems stage-matched at 24-26 cm in height (I) (n = 25). The outline of a vascular bundle is shown by a white wedge. Bars indicate S.E.M., statistical comparisons shown were made between mutant and wild-type (Student's t-test, $p < 0.001$).

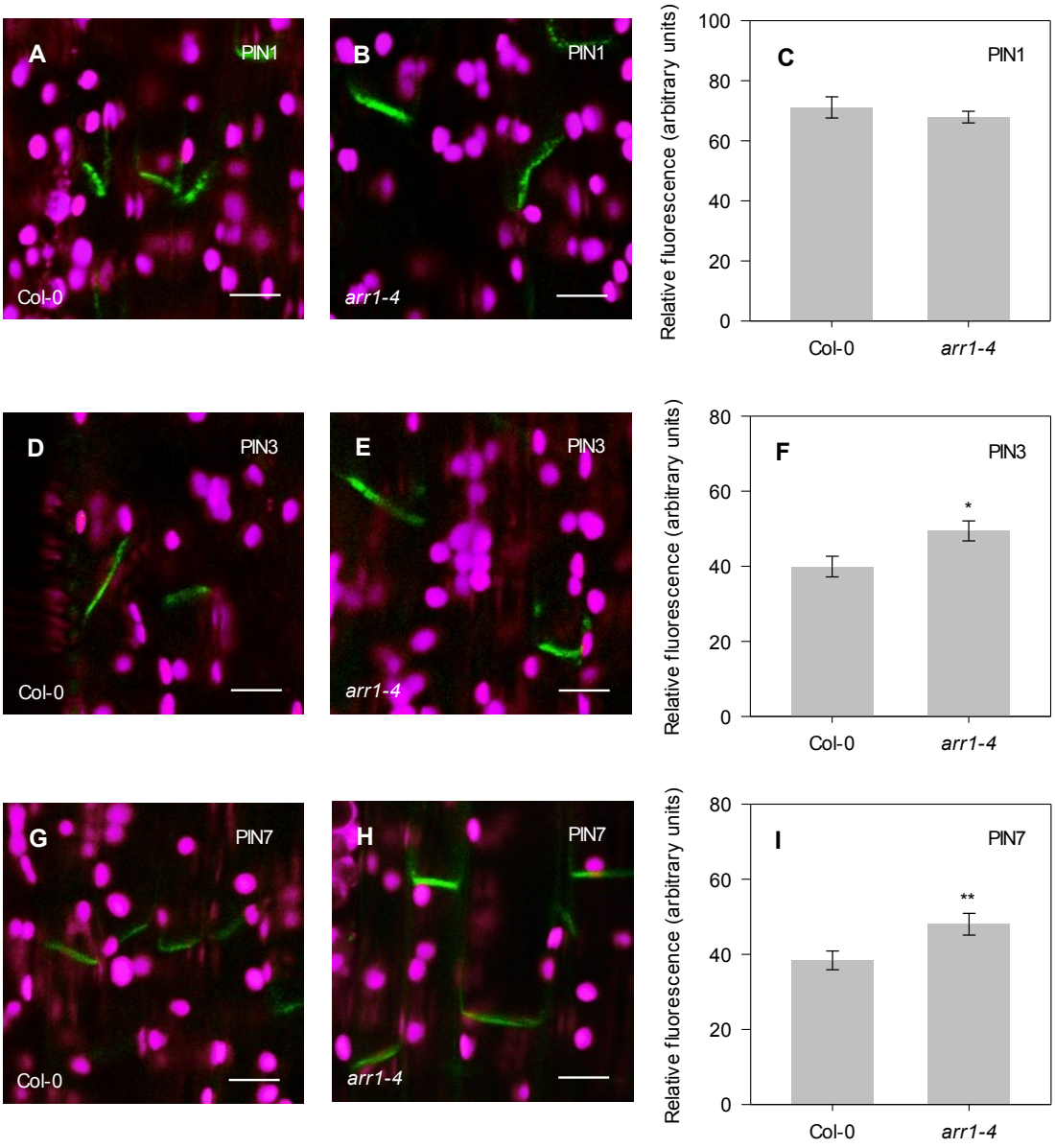

Figure 5. PIN3:PIN3-GFP and PIN7:PIN7-GFP expression is elevated in *arr1* inflorescence stems. Representative expression patterns of PIN1:PIN1-GFP (A and B), PIN3:PIN3-GFP (D and E) and PIN7:PIN7-GFP (G and H) in basal inflorescence internodes of 4-7 week old Col-0 (A, D and G) and *arr1* (B, E and H) plants, sectioned longitudinally and imaged between using confocal microscopy. Green shows PIN-GFP signal and magenta shows chloroplast autofluorescence. Scale bars represent 10 μm. The amount of GFP signal on the basal plasma membrane was

quantified in the xylem parenchyma using at least five cells each from eight independent plants (C, F and I) (n = 40). For PIN1:PIN1-GFP and PIN3:PIN3-GFP, plants were analysed at 6-7 weeks of age. For PIN7:PIN7-GFP, plants were stage-matched by comparing plants with inflorescence stems 18-20 cm in height. Bars indicate S.E.M., statistical comparisons shown were made between mutant and wild-type (Student's t-test, * = $p < 0.05$, ** = $p < 0.01$).

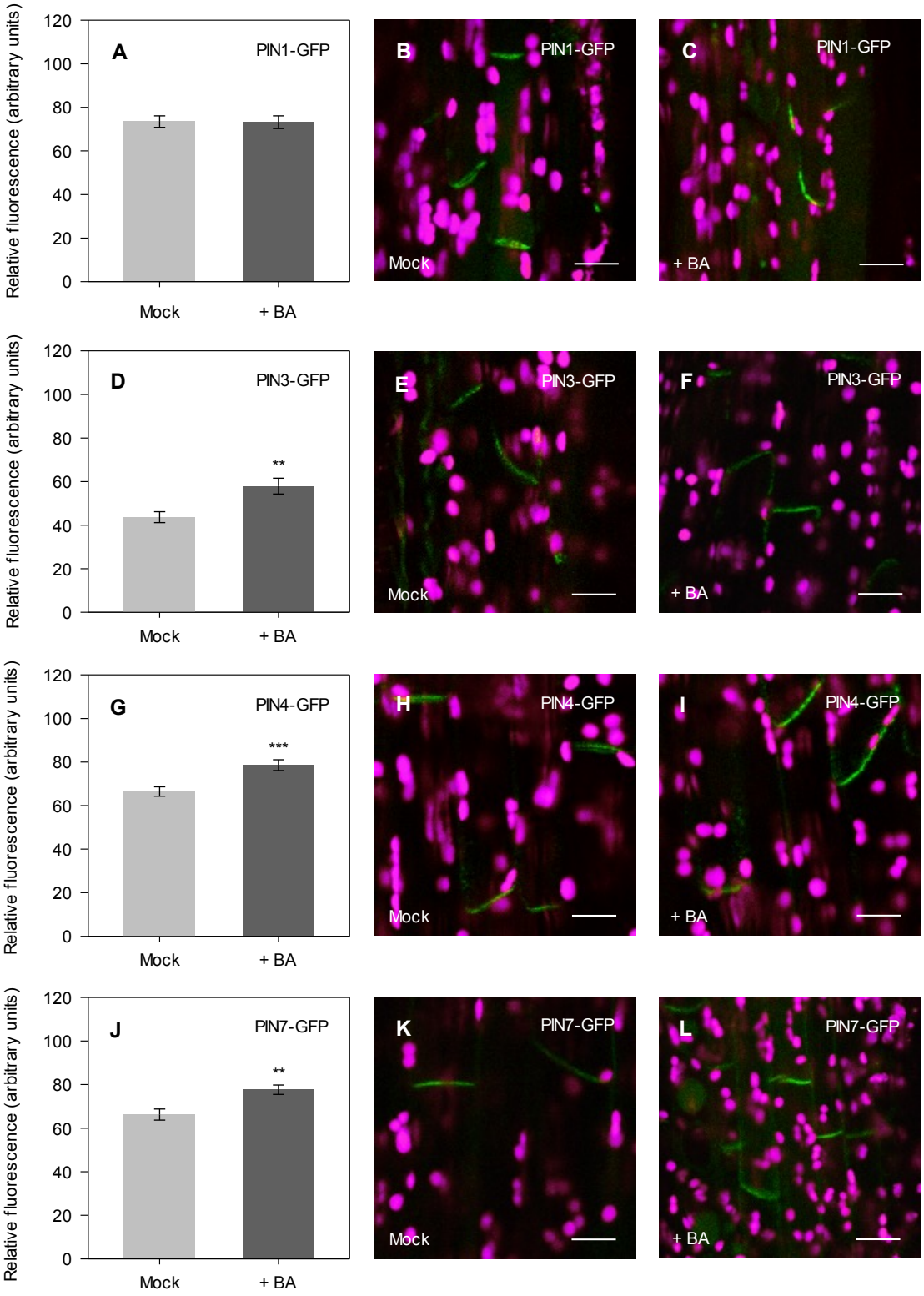

Figure 6. Cytokinin promotes the accumulation of PIN3:PIN3-GFP, PIN4:PIN4-GFP and PIN7:PIN7-GFP on the basal plasma membrane of xylem parenchyma cells in

inflorescence stems. Vertically held basal inflorescence internode segments (~2 cm) from *PIN1:PIN1-GFP* (A-C), *PIN3:PIN3-GFP* (D-F), *PIN4:PIN4-GFP* (G-I) and *PIN7:PIN7-GFP* (J-L) plants (all Col-0 background), were treated apically with 1 μM NAA and basally with either 0.1 % DMSO control ("Mock") or 1 μM BA ("+ BA"). After 4 hours, stem segments were sectioned longitudinally at their basal ends and imaged using confocal microscopy. The amount of GFP signal on the basal plasma membrane of xylem parenchyma cells was quantified in five cells each from at least seven independent plants for PIN1:PIN1-GFP (A), ten independent plants for PIN3:PIN3-GFP (D) and PIN4:PIN4-GFP (G), or eleven independent plants for PIN7:PIN7-GFP (J). Bars indicate S.E.M., statistical comparisons shown were made between mock and BA treated stems (Student's *t*-test, * = $p < 0.05$, ** = $p < 0.01$). Representative confocal images used for GFP quantifications are shown for mock (B, E, H and K) and BA (C, F, I and L) treated stems. Green shows PIN-GFP signal and magenta shows chloroplast autofluorescence. PIN1:PIN1-GFP and PIN3:PIN3GFP plants were analysed at 5-6 weeks of age. PIN4:PIN4-GFP and PIN7:PIN7-GFP plants were analysed at 4-5 weeks of age and stage-matched across treatments according to infloresence height. Scale bars represent 10 μm.

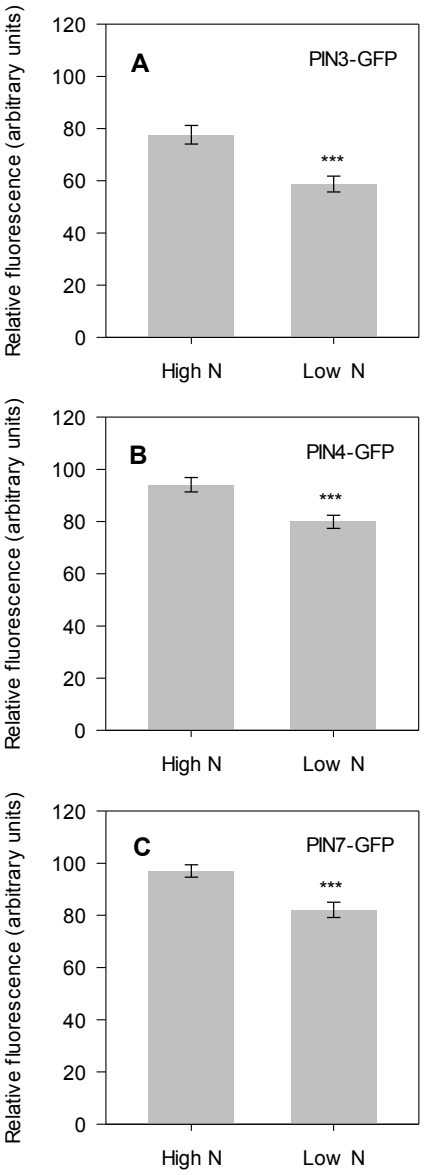

Figure 7. Growth on low nitrate (N) conditions reduces PIN-GFP accumulation. *PIN3:PIN3-GFP* (A), *PIN4:PIN4-GFP* (B) and *PIN7:PIN7-GFP* (C) plants (all Col-0 background) were grown on a sand and terragreen mix supplemented with ATS medium containing 9.0 mM NO_3 (high N) or 1.8 mM NO_3 (low N). Basal inflorescence internodes were sectioned longitudinally and imaged at 4-6 weeks of age using confocal microscopy. PIN7:PIN7-GFP plants were stage matched based on inflorescence heights across N treatments. The amount of GFP signal on the basal

plasma membrane was quantified in the xylem parenchyma using five cells each from eight independent plants for (C) (n = 40). Bars indicate S.E.M., statistical comparisons shown were made between high and low N treated plants (Student's t-test, $p < 0.001$).

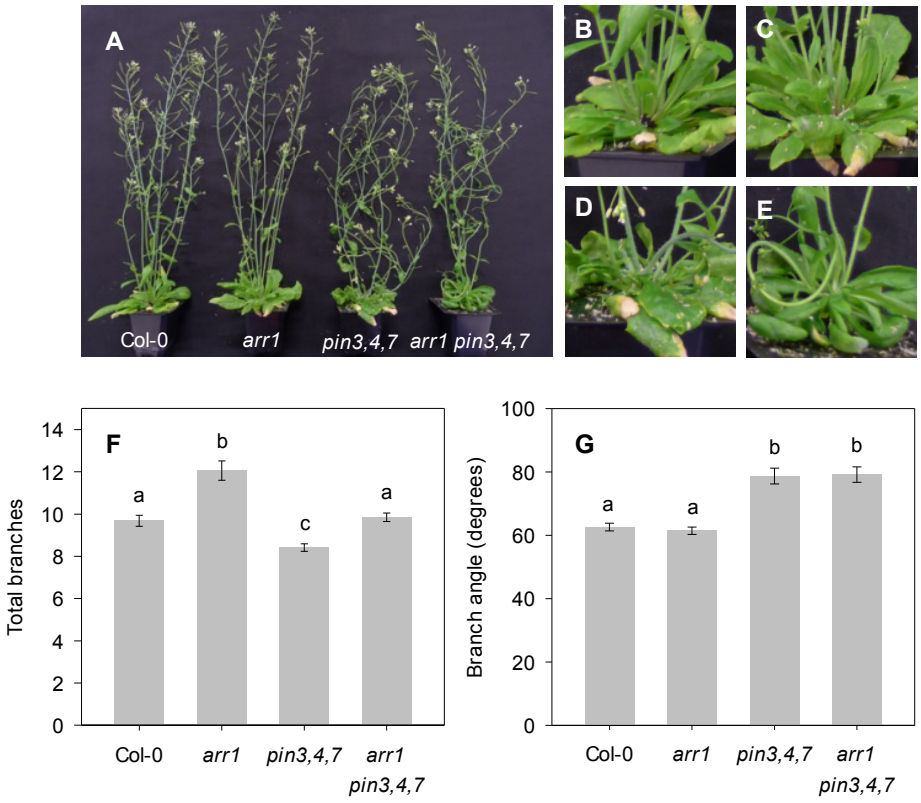

Figure 8. Interactions between *arr1* and *pin3,4,7* in shoot branching control. A-E) Shoot phenotypes of ~6 week old Col-0, *arr1*, *pin3,4,7* and *arr1 pin3,4,7* plants grown under long days. A close-up view of the rosettes in A are shown in B (Col-0), C (*arr1*), D (*pin3,4,7*) and E (*arr1 pin3,4,7*). F) Total number of branches formed at terminal flowering on ~9 week old wild-type, *arr1*, *pin3,4,7* and *arr1 pin3,4,7* plants grown under short days for 4 weeks then long days for 5 weeks (*n* = 16-47). Bars indicate S.E.M. Letters denote significant difference between genotypes (Kruskal-Wallis H test, $p < 0.05$). G) Angle between emergence point of branches on the primary inflorescence in wild-type, *arr1*, *pin3,4,7* and *arr1 pin3,4,7* plants at ~6 weeks of age. Two cauline branches were analysed per plant from at least 13 independent plants (*n* = 26-46). Bars indicate S.E.M. Letters denote significant difference (ANOVA, Tukey-b post-hoc test, $p < 0.05$).

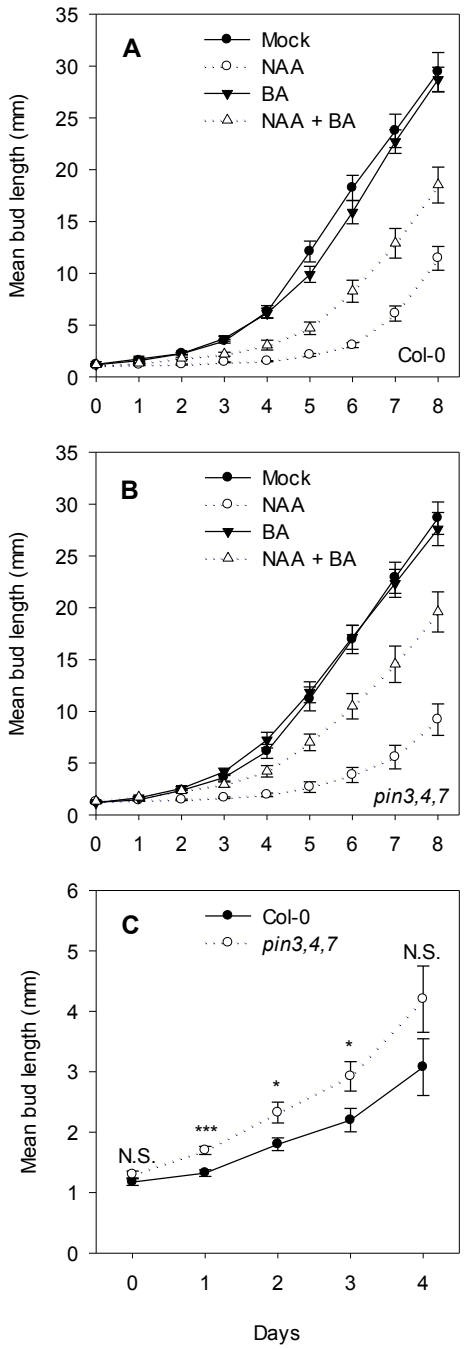

Figure 9. *pin3,4,7* exhibits altered bud activation in response to BA. Bud length of wild-type (Col-0) (A) and *pin3,4,7* (B) isolated nodal segments treated for 8 days with mock, 1 μM NAA (apical), 1 μM BA (basal) or combined 1 μM NAA (apical) and 1 μM BA (basal) (*n* = 19-20 per treatment). (C) Close-up of days 0-4 for wild-type and *pin3,4,7* buds treated with combined apical NAA and basal BA. Bars indicate S.E.M.

Asterisks denote statistically significant difference between treatments (Student's *t*-test, * = $p < 0.05$, *** = $p < 0.001$).

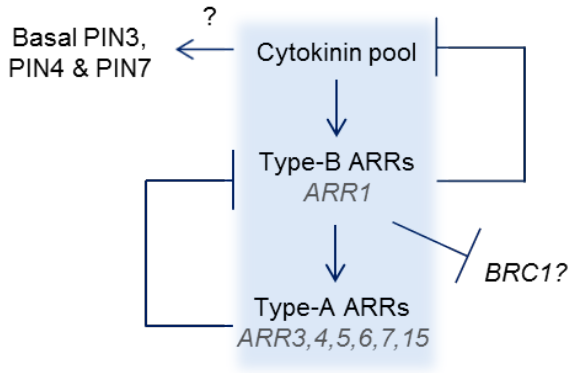

Figure 10. Proposed model for CK signalling in bud outgrowth regulation. Canonical CK signalling via the type-B *ARR1* results in feedback down-regulation of CK levels as part of signal perception. Members of the type-A *ARR* family are transcriptionally induced by *ARR1* and/or other type-B family members, and dampen type-B-mediated signalling, including the feedback down-regulation of CK levels. Basal plasma-membrane accumulation of PIN3, PIN4 and PIN7 in xylem parenchyma cells in the main stem is enhanced by CK by an unknown mechanism. In parallel, expression of other bud regulatory genes such as *BRC1* may be targeted by the canonical CK signalling pathway.

Supplemental Data

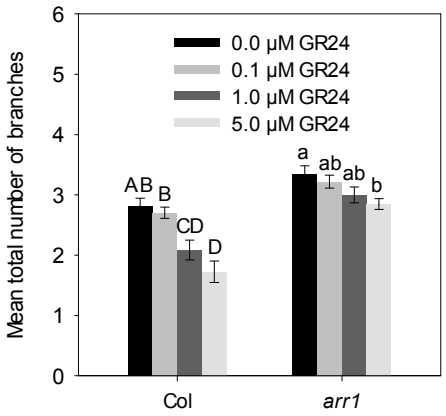

Figure S1. GR24 dose response of wild-type and *arr1*. Plants were grown for 6 weeks on different concentrations of GR24 under sterile conditions (n = 22-37). Letters denote significant difference within a genotype (Kruskal-Wallis H test, $p < 0.05$). Bars indicate S.E.M.

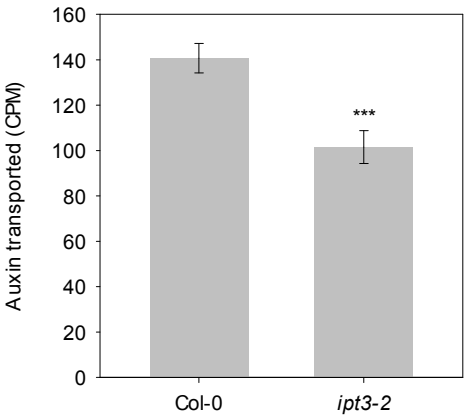

Figure S2. *ipt3* has reduced stem auxin transport. Amount of apically applied ^{14}C-IAA (counts per minute) transported to the basal end of inflorescence stem internodes from ~6 week old wild-type and *ipt3* plants in 6 hours (n = 31). Asterisks denote significant difference (Student's t-test, $p < 0.001$). Bars indicate S.E.M.

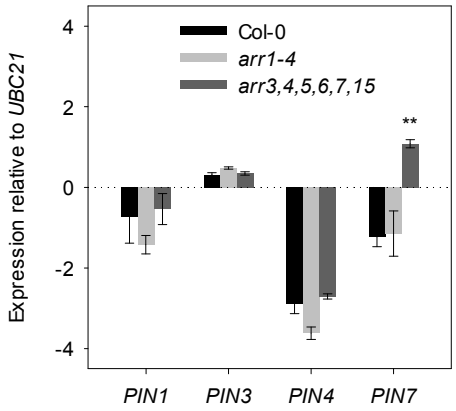

Figure S3. *PIN* gene expression in wild-type, *arr1* and *arr3,4,5,6,7,15* mutants. Expression levels shown are log-transformed and relative to *UBC21*, calculated from three biological replicates of 10-15 stems each. Bars indicate S.E.M.; asterisks denote a significant difference of a *PIN* transcript to wild-type (Student's *t*-test, $p < 0.01$).

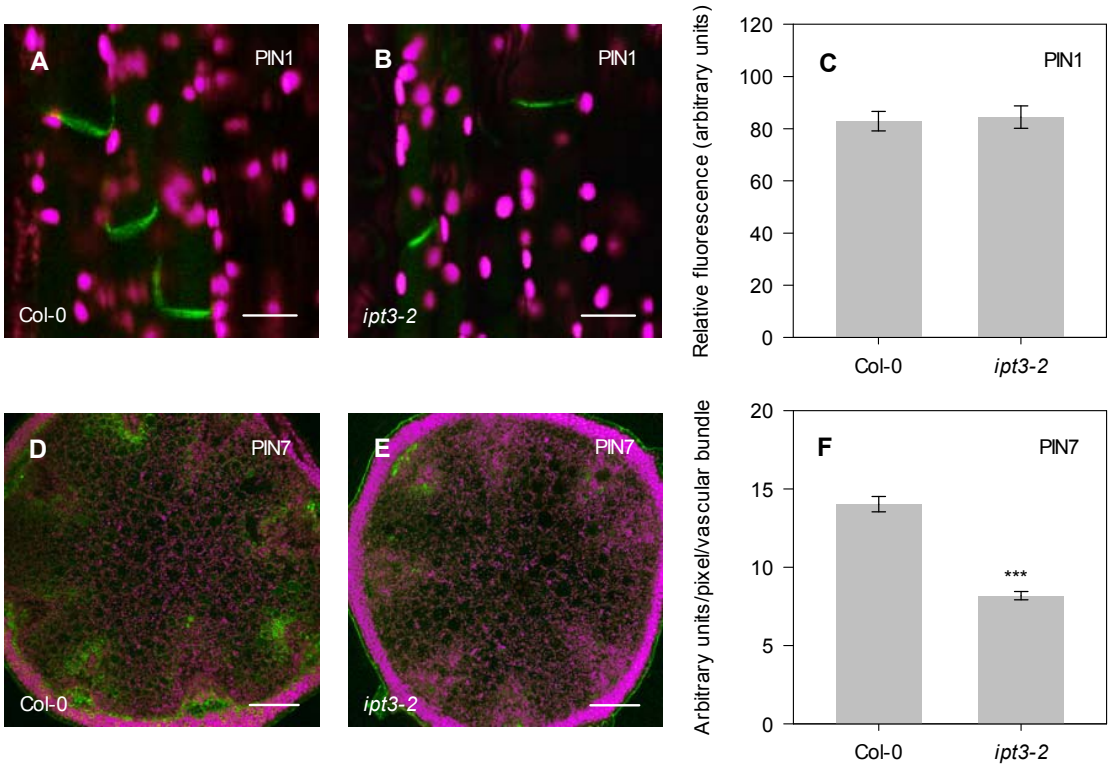

Figure S4. PIN7-GFP is reduced in *ipt3* inflorescence stems. Representative expression patterns of PIN1-GFP (A and B) and PIN7-GFP (D and E) in basal cauline internodes of Col-0 (A and D) and *ipt3-2* (B and E) plants, imaged at ~5-6 weeks of age using confocal laser microscopy. Green shows PIN-GFP signal and magenta shows chloroplast autofluorescence. Scale bars represent 10 µm (A and B) or 200 µm (D and E). For PIN1-GFP plants were sectioned longitudinally and the amount of PIN-GFP signal on the basal plasma membrane was quantified in the xylem parenchyma from at least five cells from eight independent plants (C) (n = 40). For PIN7-GFP, plants were sectioned transversely (~2 mm thickness) and the amount of PIN-GFP signal was quantified in at least five vascular bundles from eight independent plants with cauline stems stage-matched between 5-10 cm in height (I) (n = 40). Bars indicate S.E.M.; asterisks denote significant difference compared to wild-type (Student's t-test, $p < 0.001$).

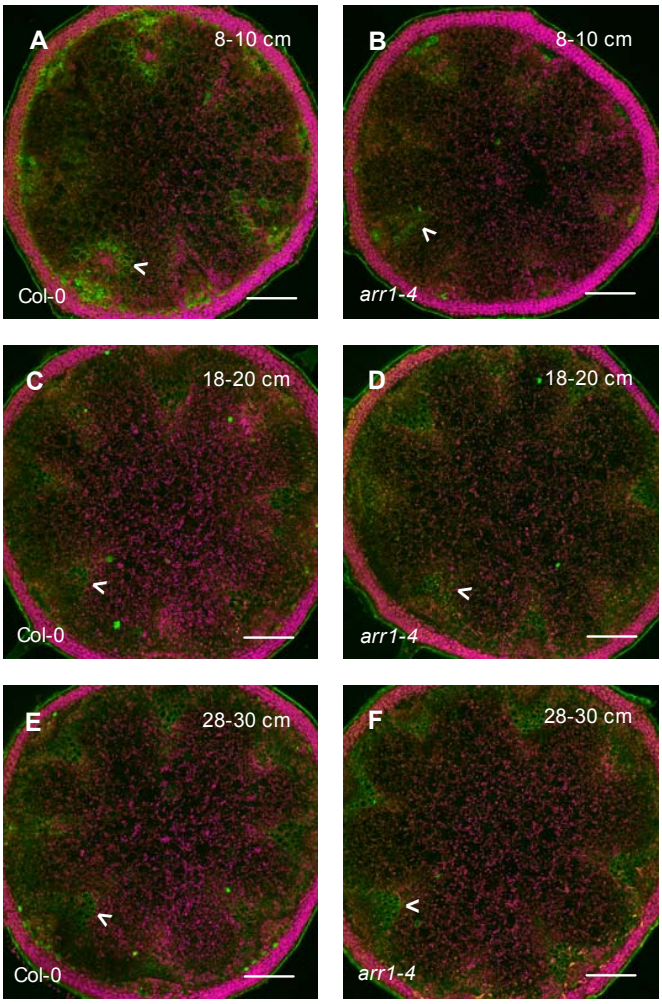

Figure S5. PIN7-GFP expression in *arr1* inflorescence stems over time. Expression patterns in ~2 mm transverse sections of basal cauline internodes from Col-0 (A, C and E) and *arr1* (B, D and F) plants with cauline stem heights of 8-10 cm (A and B), 18-20 cm (C and D) or 28-30 cm (E and F), imaged using confocal laser microscopy. Images shown are representative of at least five independent plants. White arrowheads correspond to xylem parenchyma tissue where PIN7-GFP expression is quantified. Green shows PIN-GFP signal and magenta shows chloroplast autofluorescence. Scale bars represent 200 μm.

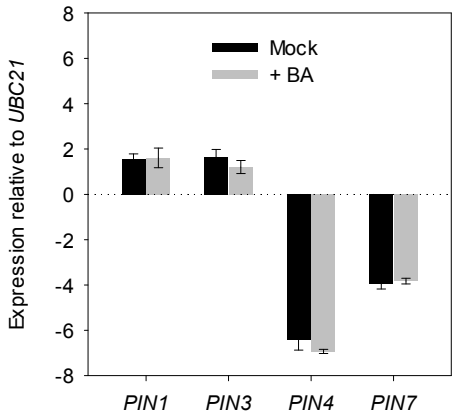

Figure S6. *PIN* gene expression is unchanged in inflorescence stems after 4 h BA treatment. Expression levels shown are log-transformed relative to *UBC21*, calculated from three biological replicates of 6 or 7 stems each. Bars indicate S.E.M. Basal cauline internode segments (~2 cm) from ~6 week old Col-0 plants were placed in split ATS-agar medium plates containing 1 µM NAA in the apical half and 0.1 % DMSO control ("Mock") or 1 µM BA ("+ BA") in the basal half. Basal 5 mm sections were harvested after 4 h hormone treatment and analysed.

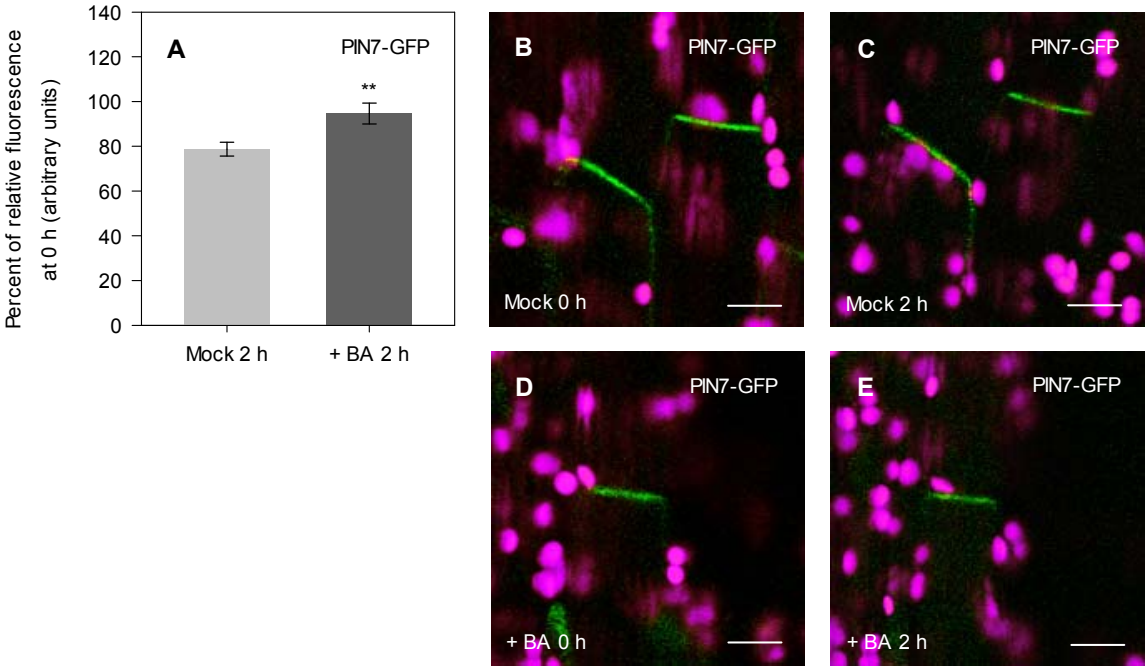

Figure S7. BA promotes accumulation of PIN7:PIN7-GFP on the basal plasma membrane of xylem parenchyma cells within 2 h. (A) The amount of GFP signal on the basal plasma membrane at 2 h was quantified using 3-5 cells each from at least 12 independent plants, calculated as a percentage of the fluorescence observed at 0 h (n = 56-59). Bars indicate S.E.M., statistical comparisons shown were made between mock and BA treated stems (Student's t-test, ** = $p < 0.01$). BA treatments were performed using basal cauline internode segments from ~4 week old PIN7:PIN7-GFP (Col-0) plants, sectioned longitudinally, treated with mock (1 µM NAA and 0.1 % DMSO control) or BA (1 µM NAA and 1 µM BA) ATS solution. Identical cells were imaged at 0 h (B and D) and 2 h (C and E) using confocal laser microscopy. Representative images used for GFP quantifications are shown for mock (B and C) and BA (D and E) treated stems. Green shows PIN-GFP signal and magenta shows chloroplast autofluorescence. Plants were stage-matched across treatments according to inflorescence height. Scale bars represent 10 µm.

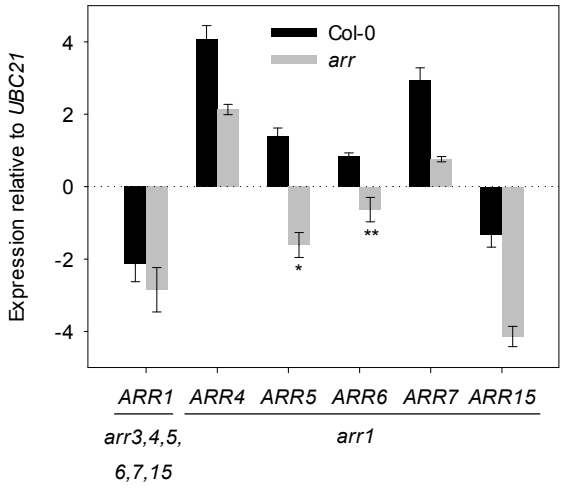

Figure S8. Expression of *ARR* genes in *arr* mutants. Expression levels shown are log-transformed and relative to *UBC21*, calculated from three biological replicates of 10-15 stems each, using *UBC21* as a reference gene. The transcript assayed within the *arr* mutant background is shown in uppercase above or in lowercase below the lines on the x-axis label, respectively. Bars indicate S.E.M.; asterisks denote significant difference to wild-type (Student's *t*-test, * = $p < 0.05$, ** = $p < 0.01$).